

~~TOP SECRET~~

~~CORONA TALENT-KEYHOLE NOFORN~~

Card (pa)



14 00029870

Total No. of Pages 70
Copy [redacted] Copies

SUMMARY REPORT

**PERFORMANCE ANALYSIS
OF THE J-3 SYSTEMS**

2 JULY 1969

Author: [redacted]

Declassified and Released by the N R C

In Accordance with E. O. 12958

on NOV 26 1997

Itek

OPTICAL SYSTEMS DIVISION

ITEK CORPORATION • 10 MAGUIRE ROAD • LEXINGTON, MASSACHUSETTS 02173

[redacted]

~~TOP SECRET~~

~~CORONA TALENT-KEYHOLE NOFORN~~

Handle Via
[redacted] TALENT-KEYHOLE
Control Systems Jointly



PREFACE

This report is basically a performance manual for the CR system.

Section 2 provides a brief description of the system in general and the panoramic cameras in more detail.

Section 3 describes the nominal design performance of the system in terms of image smear budgets and estimated GRD* numbers computed from predicted and laboratory resolution performance.

Section 4 describes the technique that has been developed for predicting GRD performance for specific targets photographed during a mission. In addition, an evaluation of the technique has been presented in this section.

In Section 5 the major parameters that affect the system performance are examined individually. This section provides some insight as to how these parameters (which are not all independent of each other) can be adjusted to optimize the system performance.

*Ground resolved distance (tri-bar target).

~~TOP SECRET~~

~~CORONA TALENT KEYHOLE NOFORN~~



CONTENTS

1.	Introduction	1-1
2.	Description of Panoramic System	2-1
2.1	General Description	2-1
2.2	Description of Panoramic Cameras	2-1
3.	Nominal System Performance	3-1
3.1	Image Smear Budgets	3-1
3.2	Nominal Resolution Performance	3-3
3.3	Predicted Performance From Laboratory Data	3-3
4.	Determination of Mission Resolution	4-1
4.1	Description of Technique	4-1
4.2	Evaluation of Technique	4-4
5.	System Evaluation	5-1
5.1	Altitude of Photography	5-1
5.2	V/h Programming Errors	5-1
5.3	Camera Smear Sources	5-1
5.4	Vehicle Effects	5-2
5.5	Lens MTF	5-5
5.6	Lens Focus	5-5
5.7	Atmospheric Effects	5-11
5.8	Exposure Time Requirements, Image Smear, and Filters	5-13
5.9	Long-Term Mission Effects	5-14
5.10	Integrated GRD	5-15
6.	Conclusions	6-1
7.	References	7-1
	Appendix — Vehicle Error Analysis for Panoramic Cameras	A-1

~~TOP SECRET~~

~~CORONA TALENT KEYHOLE NOFORN~~



Handle Via

~~TALENT KEYHOLE~~

Control Systems Jointly

~~TOP SECRET~~

CORONA ~~TALENT-KEYHOLE-NOFORN~~



FIGURES

2-1	Camera Module, Supply End	2-4
2-2	Camera Module, Takeup End	2-5
2-3	J-3 Camera System	2-6
2-4	Configuration and Orientation	2-7
2-5	View of Camera From Outboard Side	2-9
2-6	View of Camera From Inboard Side	2-10
2-7	Closeup View of Lens Focal Plane Area	2-11
2-8	Panoramic Lens Assembly and Rails	2-12
5-1	Cross-Track Smear, AFT-Looking Camera	5-3
5-2	Cross-Track Smear, FWD-Looking Camera	5-4
5-3	MTF's for Lenses I-215 and I-192	5-6
5-4	MTF's of Lens I-215, III Generation Lens With 3404 Film	5-7
5-5	MTF's of Lens I-215, III Generation Lens With 3404 Film and Wratten No. 25 Filter	5-8
5-6	MTF's of Lens I-192, II Generation Lens With 3404 Film and Wratten No. 21 Filter	5-9
A-1	X Definition	A-5
A-2	Y Definition	A-5
A-3	Panoramic Camera Format	A-5

~~TOP SECRET~~

CORONA ~~TALENT-KEYHOLE-NOFORN~~



Handle Via

~~TALENT-KEYHOLE~~

Control Systems Jointly



TABLES

2-1	Summary of Physical Features and Operational Parameters	2-8
3-1	Cross-Track Image Smear Budget, 2.44-Millisecond Exposure, 3 σ Values, 3404 Film	3-4
3-2	Along-Track Image Smear Budget, 2.44-Millisecond Exposure, 3 σ Values, 3404 Film	3-5
3-3	Predicted System Performance, 80 nm, 2 σ Values, 0-Degree Field, 2:1 Contrast, 2.44-Millisecond Exposure, 3404 Film, II Generation Lens With Wratten No. 21 Filter	3-6
3-4	Predicted System Performance, 80 nm, 2 σ Values, 0-Degree Field, 2:1 Contrast, 3.64-Millisecond Exposure, 3404 Film, III Generation Lens With Wratten No. 25 Filter	3-7
3-5	Laboratory Resolution Tests at Center of Format	3-8
4-1	CORN Target Resolution, Comparison of Readings and Predictions, Mission 1101, FWD-Looking Camera, Low Contrast (2:1)	4-8
4-2	CORN Target Resolution GRD, Comparison of Readings and Predictions, Mission 1101, AFT-Looking Camera	4-9
4-3	CORN Target Readings and Predictions, Mission 1102, FWD-Looking Camera	4-10
4-4	CORN Target Readings and Predictions, Mission 1102, AFT-Looking Camera	4-11
4-5	CORN Target Readings and Predictions, Mission 1103	4-12
4-6	CORN Target Readings and Predictions, Mission 1104	4-13
5-1	Statistics of V/h Programming Errors	5-3



1. INTRODUCTION

The contractor has conducted a study of the performances of the panoramic systems which were utilized in missions 1101 through 1104. (The 1100 series panoramic system is described in Section 2.) The results of the study have been published in the following reports:

1. Performance Analysis Report for Mission 1101^{1*}
2. Performance Analysis Report for Mission 1102²
3. Performance Analysis Report for Mission 1103³
4. Performance Analysis Report for Mission 1104⁴.

The present report summarizes the findings of the study for all four missions and attempts to convey some insight into the effects on system performance of the various physical parameters.

*References are listed in Section 7.



2. DESCRIPTION OF PANORAMIC SYSTEM

2.1 GENERAL DESCRIPTION

The panoramic camera system consists basically of two panoramic cameras forming a stereoscopic pair at an angle of convergence of 30 degrees (approximately). Both cameras, as well as several electronics packages, are mounted on a single supporting structure. The film supply for the whole mission is contained in a cassette mounted on a separate supporting structure. Figs. 2-1 and 2-2 are photographs of the whole system described above. In Fig. 2-1, the film supply cassette is visible. The cassette contains two large spools, one for each panoramic camera. Fig. 2-3 shows the location of the panoramic system inside the orbiting vehicle. Two recovery vehicles, each containing two takeup spools, are also shown in Fig. 2-3. The recovery vehicles are located forward of the panoramic system. The Agena section of the vehicle mounted aft of the panoramic system is not shown. Fig. 2-4 depicts in schematic form the configuration of the panoramic system. Table 2-1 summarizes the physical features and operational parameters of the system.

One of the panoramic cameras is pointed approximately 15 degrees from the local vertical in the direction of vehicle flight (FWD-looking camera). The other panoramic camera is pointed approximately 15 degrees from the local vertical in a direction opposite to the direction of flight (AFT-looking camera).

The orbit usually has an inclination of approximately 80 degrees (an almost polar orbit). Most of the photographic coverage is concentrated in the northern hemisphere and is obtained while the vehicle is descending from the northern latitudes towards the equator. The first priority targets (otherwise denoted as HPL targets in this report) have an average latitude of approximately 50°N and a standard deviation of approximately 7 degrees. The geographic location of these targets affects the altitude of photography as well as the exposure times required. Thus, it affects the panoramic system's performance (see Sections 5.1 and 5.8).

The panoramic cameras are mechanically identical. However, they usually carry slightly different lenses and filters. Most of the FWD-looking cameras are equipped with third generation Petzval lenses and Wratten no. 25 filters, while the AFT-looking cameras are equipped with second generation Petzval lenses and Wratten no. 21 filters. Systems 1101, 1102, and 1103 were exceptions to this rule because their FWD-looking cameras were equipped with second generation lenses.

2.2 DESCRIPTION OF PANORAMIC CAMERAS

Figs. 2-5, 2-6, and 2-7 are photographs of a single panoramic camera. The panoramic camera consists of a complete lens assembly and a main structure. The lens is enclosed in a cylindrical drum approximately 48 inches in diameter. Two diametrically located openings in the drum permit light to enter and exit the lens. In Fig. 2-7, one of the openings, as well as the

~~TOP SECRET~~

~~CORONA TALENT KEYHOLE NOFORN~~

focal plane portion of the lens, is visible. In Fig. 2-5, the drum is clearly visible and a portion of the lens can be seen through one of the removable service covers on the drum.

The lens assembly and the drum rotate counterclockwise (see Fig. 2-5) with a constant angular velocity. The mechanical axis of rotation passes (approximately) through the vacuum rear node of the lens. The significance of the rear node of the lens is that for targets located at infinity, their images are stationary in space when the lens rotates through its rear node. The field of view in the along-track direction (approximately parallel to the direction of flight) is approximately 5 degrees. In the cross-track direction, the field of view is smaller and variable depending on the width of the slit in the focal plane. Thus, at any instant of time, only the images of targets that are located within a small angular field are visible in the focal plane. However, the scanning motion of the lens extends the useful field of view in the cross-track direction to approximately 70 degrees. Therefore, the panoramic format covers a field of view of approximately 5 by 70 degrees. During exposure of a panoramic frame, the film is maintained stationary in the shape of a section of a cylinder whose radius equals the focal length of the lens and whose axis coincides (approximately) with the scanning axis. The film is forced into the cylindrical shape by tension and is supported by rollers on the drum and the focal plane of the lens (visible in Fig. 2-7) as well as two cylindrical rails mounted on the film transport assembly (shown in Fig. 2-5). One of the rails is also visible in Fig. 2-7. Fig. 2-8 shows in schematic form the Petzval lens and the rails during exposure of the center of format. The exposure time of the film is controlled by the scanning speed of the lens and the width of the slit.

Since the vehicle is moving forward along its trajectory with a certain velocity, the constant scanning speed of the lens must be such that successive frames cover adjacent areas on the ground with a certain amount of overlap. In fact, it can be shown that the scanning speed is directly proportional to V/h (ratio of vehicle velocity to altitude). Furthermore, because of the forward motion of the vehicle, the images of ground targets are moving primarily in the along-track direction. If this motion was not compensated, the panoramic frames would be smeared badly in the along-track direction. However, if the film was moving with the same velocity as the image during exposure, no image smear would result. In fact, this is being accomplished by rotating the whole panoramic camera about an axis parallel to the pitch axis of the vehicle. While a frame is being exposed, the camera is rotating about this axis with an angular velocity proportional to V/h . Fig. 2-6 shows the axis of rotation which is identified as forward motion compensation (FMC). Most of the image motion in the along-track direction is compensated in this fashion. There is, however, some image motion in the cross-track direction which is due to the forward motion of the vehicle and the stereo convergence angle. This image motion is not being compensated and is identified as the uncompensated cross-track image motion. Rotation about the FMC axis is not continuous but reciprocating, so it becomes necessary to synchronize the scanning action of the lens with rotation about the FMC axis. Rotation about the scanning axis is accomplished by utilizing a single torque motor which rotates the lens and drum assembly. Rotation about the FMC axis is achieved with an FMC cam attached to the motor drive shaft. The speed of the motor is controlled through a closed-loop servo. In turn, the servo is controlled by a voltage input from the V/h programmer. This voltage is proportional to the required V/h rate. The servo responds by causing the torque motor to rotate at a speed proportional to the input voltage. Hence, the scanning speed of the lens is proportional to V/h . The constant of proportionality is fixed and is such that approximately 7.6 percent overlap is maintained between successive frames at the center of the panoramic format. The torque motor and tachometer (speed-sensing device of the servo) are visible in Fig. 2-6.

~~TOP SECRET~~

~~CORONA TALENT KEYHOLE NOFORN~~

Handle Via

~~TALENT KEYHOLE~~

Control Systems Jointly

~~TOP SECRET~~

~~CORONA TALENT-KEYHOLE NOFORN~~

A lens cycle is a complete revolution of the lens. The photographic part of the lens cycle is the exposure of the panoramic format (70 degrees of scan angle rotation out of 360 degrees). The FMC cam is designed so that during the photographic part of the lens cycle, the speed of rotation of the camera about the FMC axis is proportional to the scanning speed of the lens. The constant of proportionality (otherwise known as the cam constant) is nominally 0.01321. Thus, while a panoramic frame is being exposed, the FMC rate is approximately equal to the V/h rate.

After a panoramic frame has been exposed, the lens rotates approximately 290 degrees before the exposure of another frame begins. During this part of the lens cycle, the exposed frame is transported toward the takeup spool and a new frame is introduced into the format area (rails).

Each panoramic camera is also equipped with two horizon frame cameras. One of these units is visible in Figs. 2-5, 2-6, and 2-7.

The Petzval lens is equipped with a filter tray containing two filters. During the mission, either one of the two filters could be selected to filter the light which illuminates the film. The exposure of the film is controlled by varying the slit width. The mechanism by which the slit width is varied during the mission allows the selection of one out of four predetermined slit widths. In Fig. 2-7, the mechanisms for changing the filters and the slit width are visible. In addition, in Fig. 2-7 four rollers are visible in the focal plane area of the lens. Of these, the two rollers in the center (nearest to the lens slit) establish the focal plane of the lens and are defined as the focal plane rollers.

This description of the panoramic system is by no means complete. However, a more detailed description⁵ is beyond the scope of this report.

~~TOP SECRET~~

~~CORONA TALENT-KEYHOLE NOFORN~~

Handle Via

~~TALENT-KEYHOLE~~

Control Systems Jointly

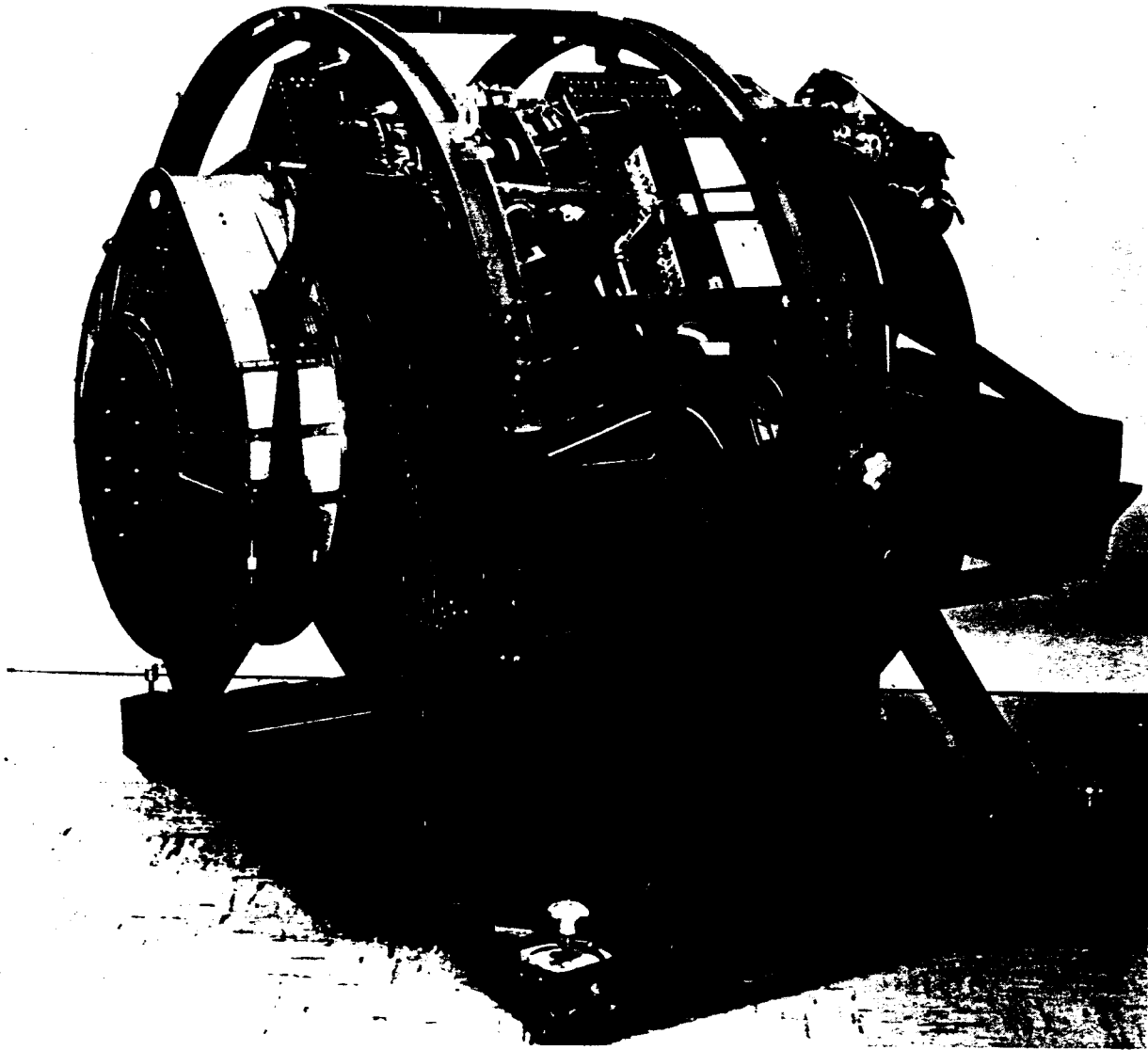


Fig. 2-1 — Camera module, supply end



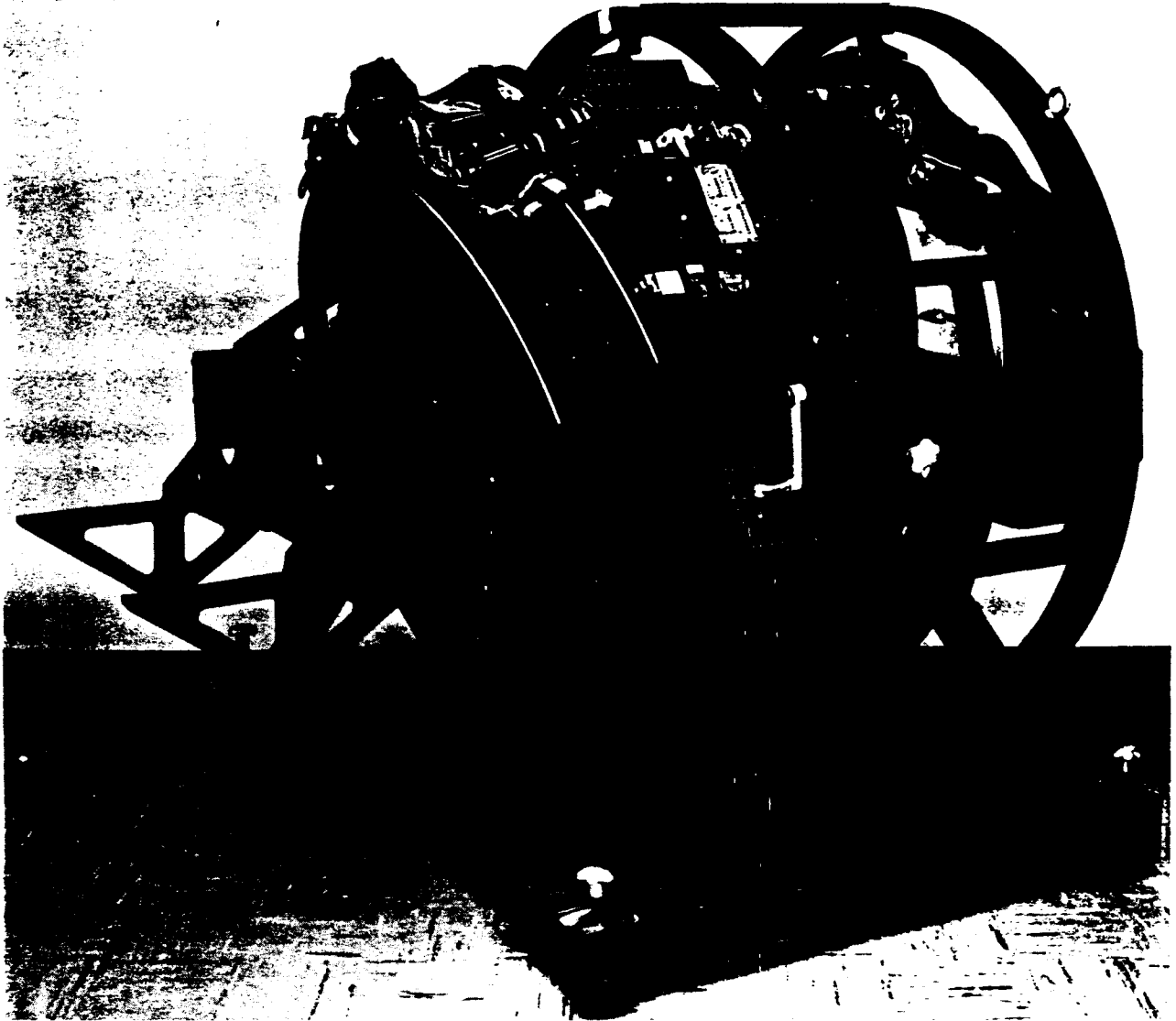


Fig. 2-2 — Camera module, takeup end



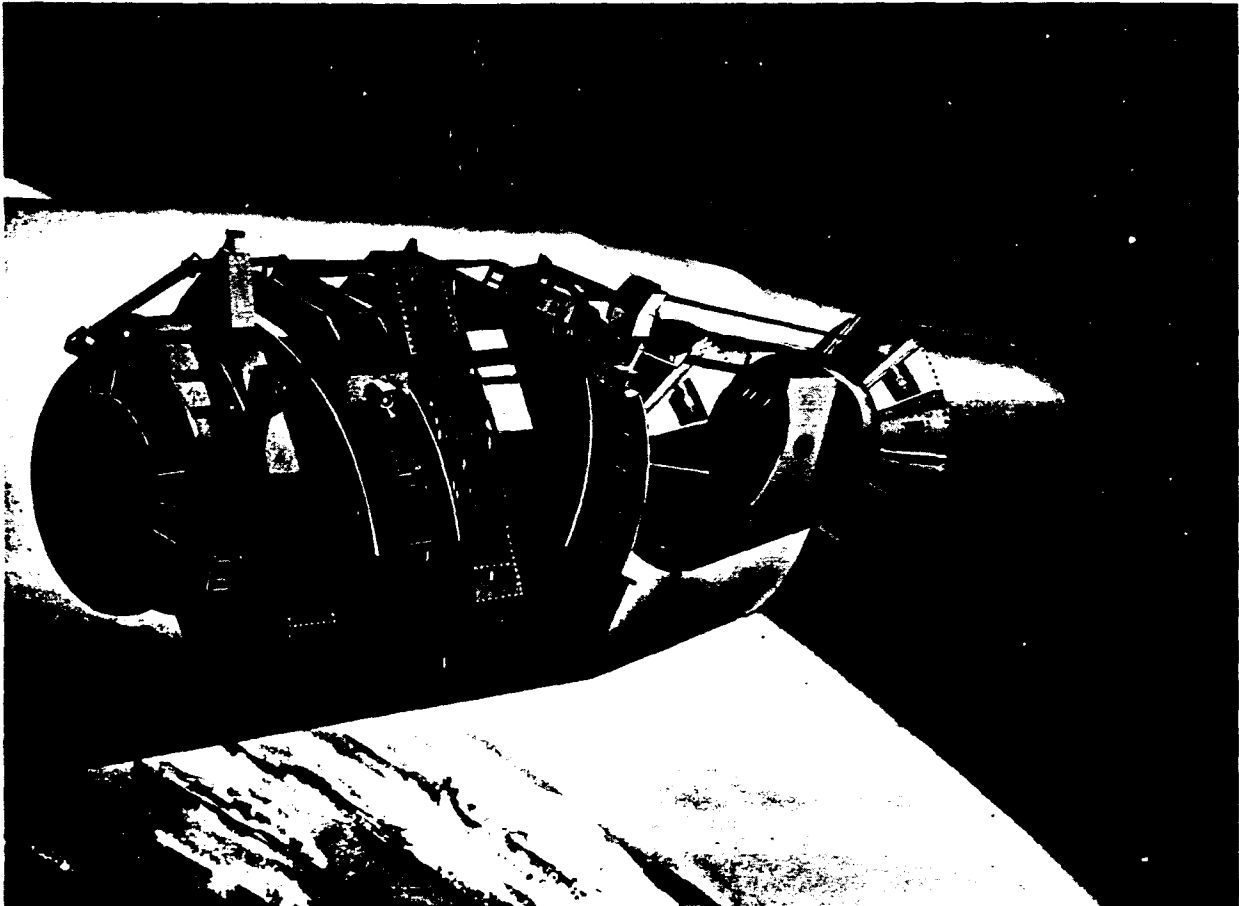


Fig. 2-3 — J-3 Camera System

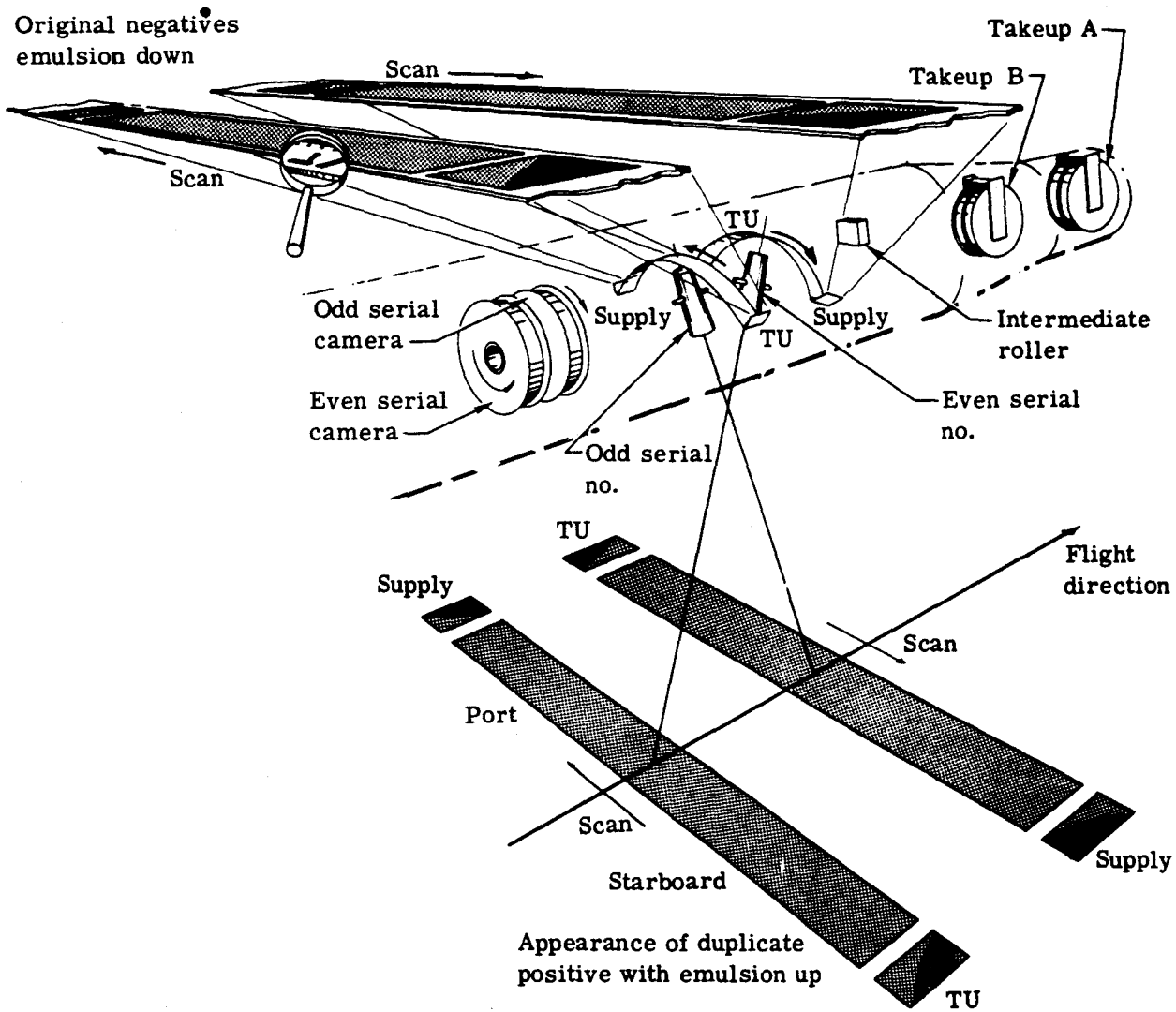


Fig. 2-4 — Configuration and orientation



Table 2-1 — Summary of Physical Features and Operational Parameters

Physical Features

Configuration	30-degree convergent stereo panoramic cameras
Lenses	24-inch focal length, f/3.5 Petzval design
Film capacity	16,000 feet of 70-millimeter, 3.0-mil, polyester-base film per camera
Film size	31.632 × 2.754 inches
Usable format	29.323 × 2.147 inches
Weight (empty)	Approximately 437 pounds
Weight (with film)	Approximately 597 pounds
Cycle period	1.5 to 4.2 seconds per cycle
Exposure time	Variable
Overlap	Fixed at 7.6 percent
Filter	Variable (2-position)

Operational Parameters

V/h range	0.0525 to 0.021 radian per second
Altitude	80 to 200 nm
Cross-track coverage per frame	116 to 290 nm
Along-track coverage per frame	7.73 to 19.33 nm
Total along-track coverage	41,820 nm at 80-nm altitude
Total operating time	172 minutes at 80-nm altitude

~~TOP SECRET~~

~~CORONA TALENT KEYHOLE NOFORN~~

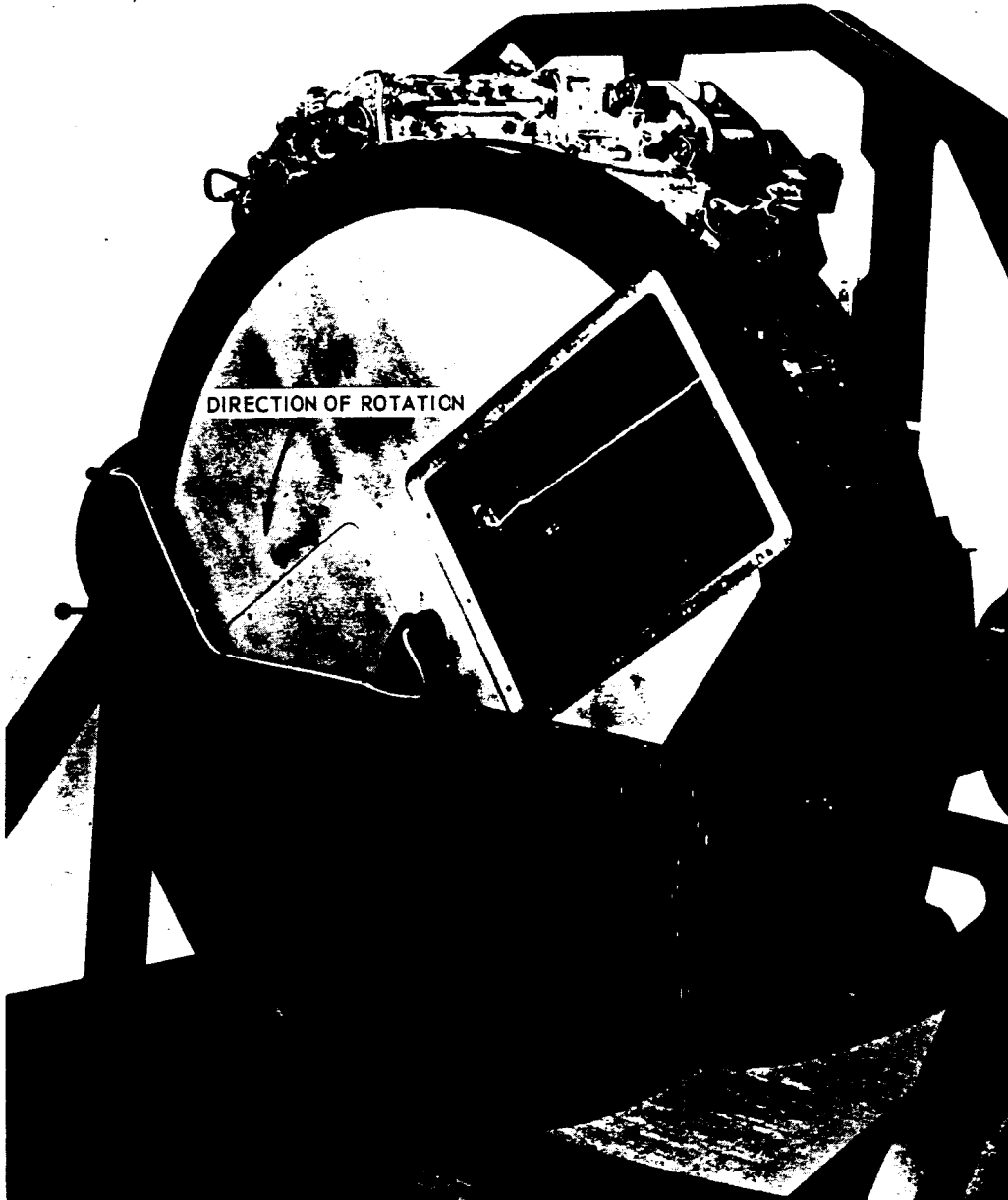


Fig. 2-5 — View of camera from outboard side

~~TOP SECRET~~

~~CORONA TALENT KEYHOLE NOFORN~~



Handle Via

~~TALENT KEYHOLE~~

Control Systems Jointly

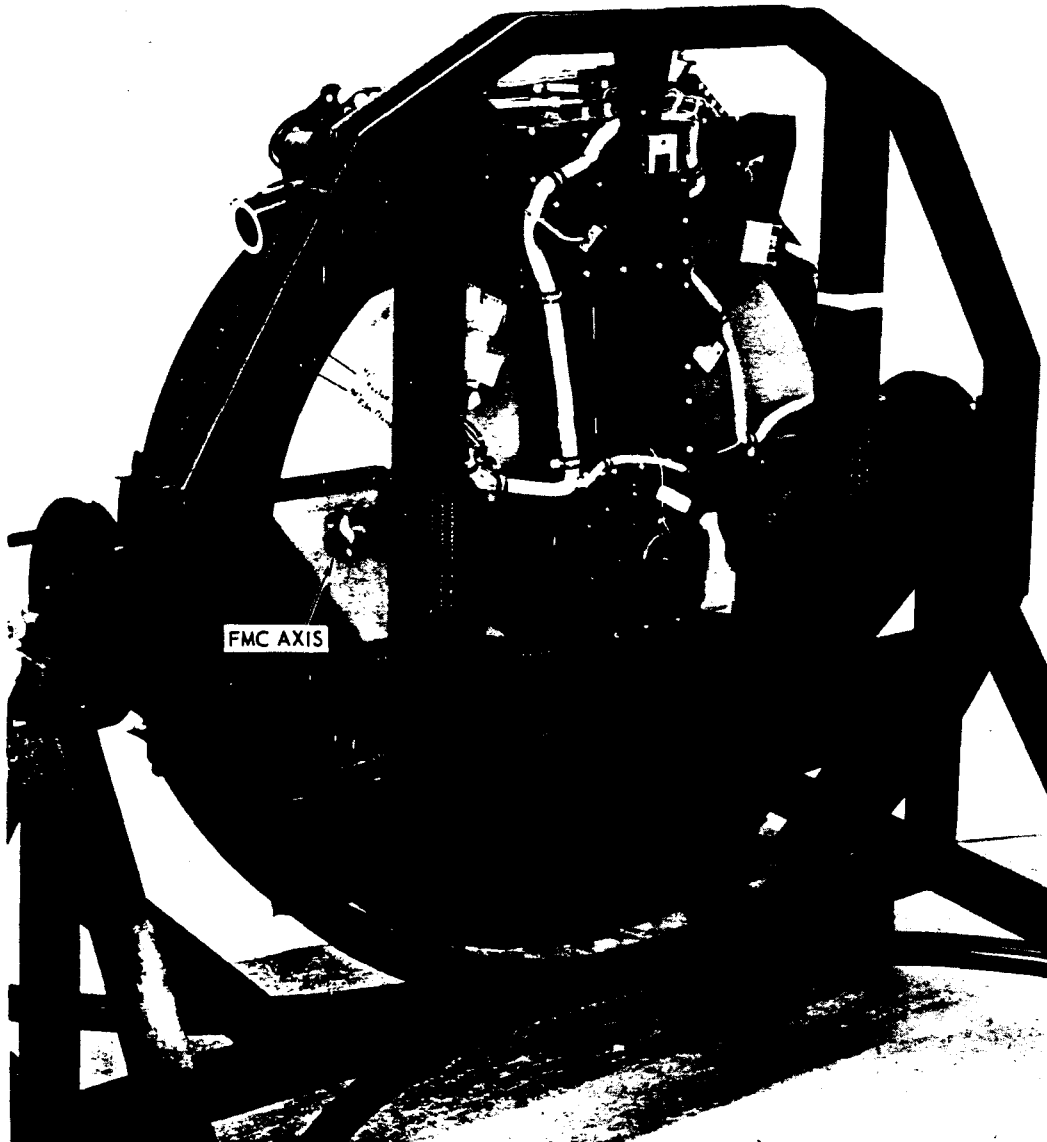


Fig. 2-6 — View of camera from inboard side

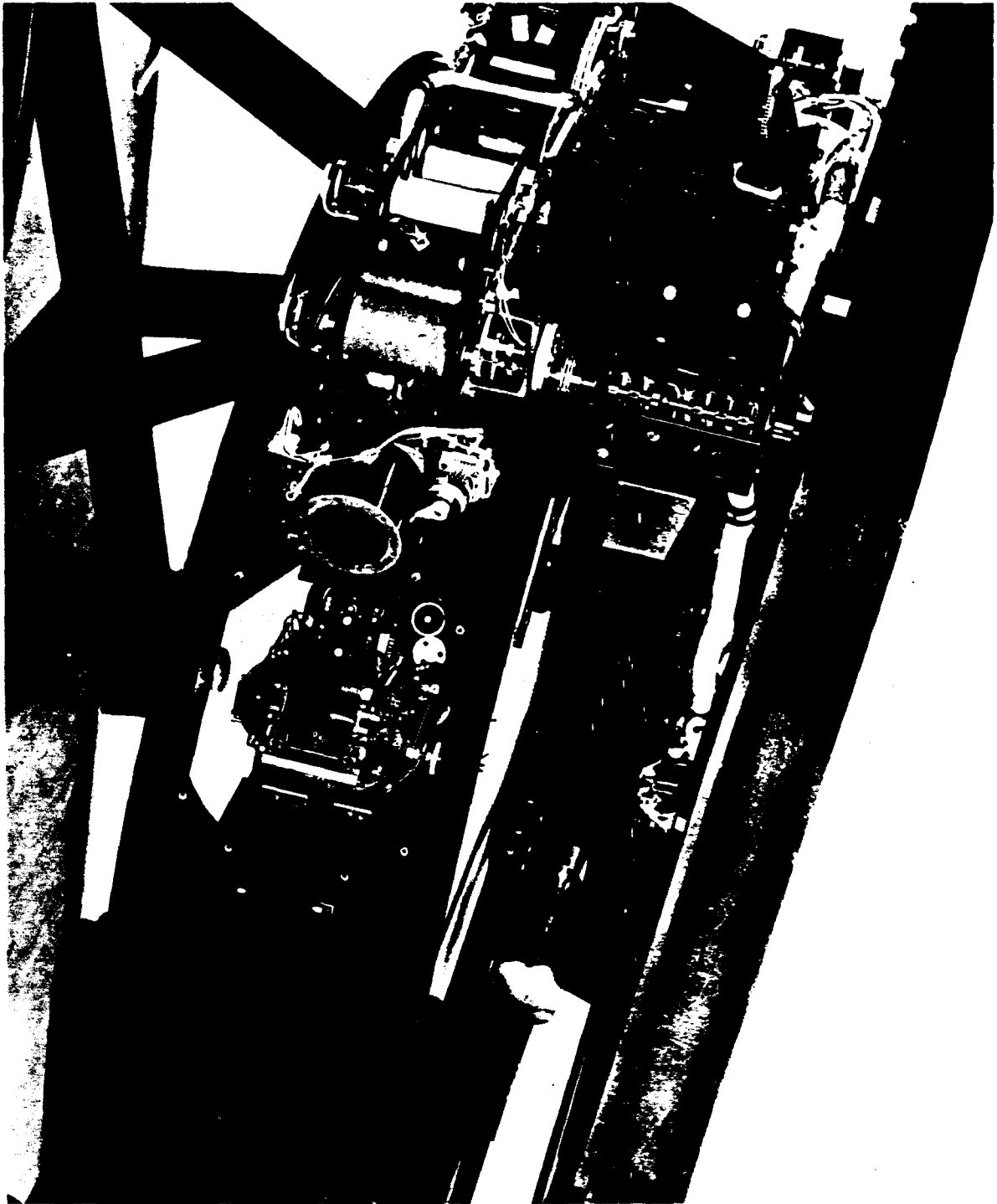


Fig. 2-7 — Closeup view of lens focal plane area



~~TOP SECRET~~

~~CORONA TALENT KEYHOLE NOFORN~~

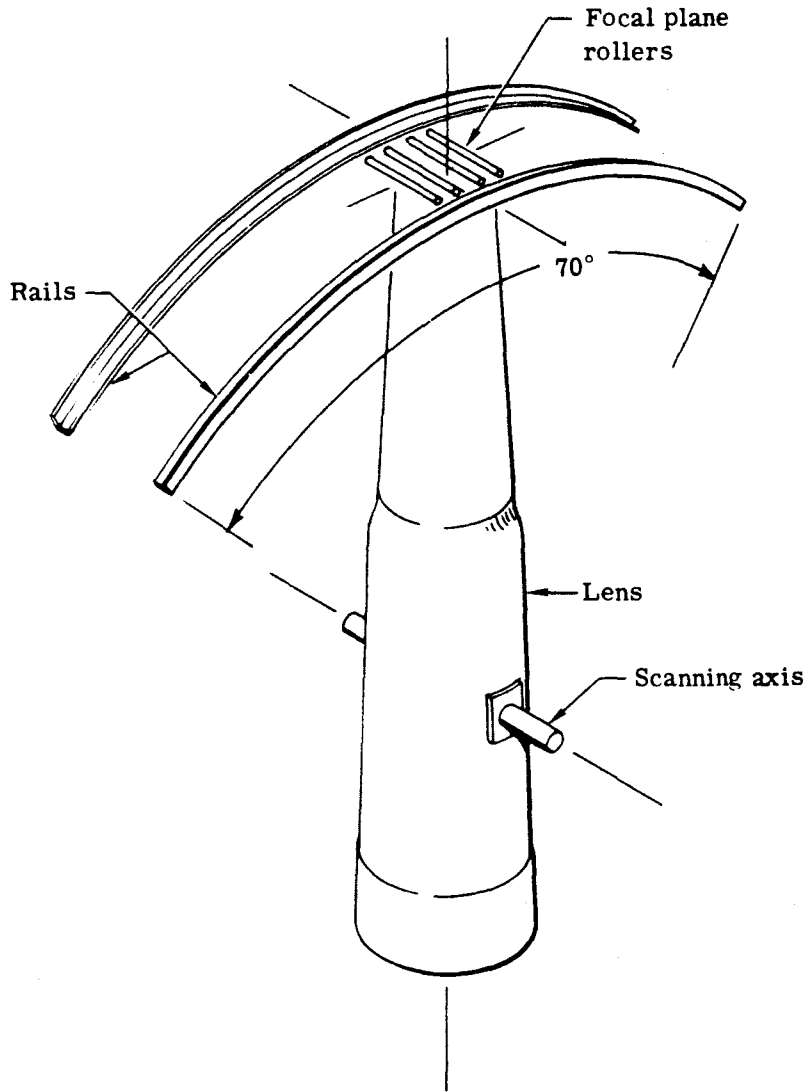


Fig. 2-8 — Panoramic lens assembly and rails

~~TOP SECRET~~

~~CORONA TALENT KEYHOLE NOFORN~~



Handle Via

~~TALENT KEYHOLE~~

Control Systems Jointly



3. NOMINAL SYSTEM PERFORMANCE

3.1 IMAGE SMEAR BUDGETS

The camera is basically a device which records three-dimensional objects into two-dimensional photographic images. This recording process is known to be imperfect since only a portion of the information present in an object is recorded. Obviously, some information is lost when a three-dimensional object is recorded as a two-dimensional image. In aerial and space photography with a vertically pointed camera, most of the height information of ground objects is lost. To circumvent this difficulty in the panoramic system, two panoramic cameras which form a stereoscopic pair are utilized. Thus, the height information is partly recovered by obtaining two stereoscopic images of the same object.

However, the most significant loss of information results from a basic physical property of a camera, i.e., that each point of an object is recorded as a spot of finite size on the film. The image of a point at infinity (e.g., a star) formed by the optics has a light intensity distribution described by the well known spread function. This image when recorded on film is further enlarged and distorted by the film.

This physical property of a camera to record points in the object space into spots of finite size causes the very small detail of a real ground target to be badly distorted and unrecognizable in the photographic image. Of course, the type of detail which is barely recognizable depends on the camera system utilized and the altitude of photography. However, all cameras are known to be unable to record information contained in spatial frequencies larger than a cutoff frequency (cycles per millimeter on the film). Information contained in the passband (spatial frequencies lower than the cutoff frequency) is recorded with various amounts of distortion. The cutoff frequency and the performance in the passband varies with camera design and photographic system* operating characteristics.

The panoramic system's performance is directly affected by the following parameters:

1. Atmosphere
2. Lens performance
3. Film focus position
4. Image smear
5. Film quality.

Since the lens is the image-forming part of the system, the lens performance is the upper limit to the performance of the panoramic system. The other parameters (atmosphere, film focus position, image smear, film quality) tend to degrade the system's performance to a level lower

* The photographic system's performance depends on the camera performance as well as atmospheric effects and vehicle motions.

~~TOP SECRET~~

~~CORONA TALENT KEYHOLE NOFORN~~

than that of the lens performance. For that reason, these parameters, with the exception of the atmosphere, are tightly controlled. In addition, all of the parameters listed above, with the exception of the atmosphere, are affected by the mission environment. In Section 5 of this report, a more detailed discussion of environmental and mission parameters which directly or indirectly (by modifying the five basic parameters presented above) affect system performance is presented.

The criterion of performance in the design and testing of the panoramic cameras is the well known tri-bar resolution. The lenses were tested statically in an optical bench and accepted only if they would produce the following low-contrast (2:1) resolution numbers:

1. 140 lines per millimeter (minimum) for second generation lenses with a Wratten no. 21 filter and 3404 film
2. 180 lines per millimeter (minimum) for third generation lenses with a Wratten no. 25 filter and 3404 film.

Then each camera was tested dynamically and accepted if it produced the following low-contrast (2:1) resolution numbers on 3404 film:

1. 110 lines per millimeter (minimum) for cameras equipped with a second generation lens and a Wratten no. 21 filter
2. 150 lines per millimeter (minimum) for cameras equipped with a third generation lens and a Wratten no. 25 filter.

It should be mentioned that tri-bar resolution does not fully describe the performance of photographic systems, mainly because the image-forming qualities of the lenses or optics employed cannot be described fully by tri-bar resolution. Thus, if two photographic systems employing optics of different designs were compared on the basis of tri-bar resolution, some erroneous conclusions might be reached. However, lenses of the same design could be compared with each other on an approximate and relative basis by determining their tri-bar resolutions with specific films. The lens performance can be very well described by its modulation transfer function (MTF). For a long time, a reliable and practical technique for measuring the MTF of a lens did not exist. At the present time, however, the measurement of lens MTF's by the laser unequal path interferometer is a routine procedure in the contractor's laboratories. The MTF of a lens is so valuable for describing its behavior that it is anticipated that the sophisticated optics of the future will be specified, tested, and accepted on the basis of their MTFs.

On the other hand, the concept of the modulation transfer function is not considered to be very useful as a performance criterion for photographic systems because it does not account for the noise generated by the grain structure of photographic images. In addition, the MTF concept is mathematically meaningless for a photographic system because of the nonlinear response of the film.

The Petzval lenses were designed to give the static resolution values mentioned above, and the final lens design was determined in the following manner. For any specific lens design the corresponding static resolution value was predicted from the lens MTF. Then the lens design was altered until the desired static resolution values could be predicted from the resulting lens MTF. After the final lens design was established, it became necessary to control the film focus position and the allowable image smear so that the dynamic camera resolution would be maintained above the levels indicated on page 3-2. Since image smear arises from many sources, image smear

~~TOP SECRET~~

~~CORONA TALENT KEYHOLE NOFORN~~

Handle Via

~~TALENT KEYHOLE~~

Control Systems Jointly



budgets were constructed and are shown in Tables 3-1 and 3-2. Only the major sources of image smear are included in Tables 3-1 and 3-2. During the design of the panoramic system the most significant image smear sources were controlled to the levels shown in the budgets.

3.2 NOMINAL RESOLUTION PERFORMANCE

The image smear budgets shown in Tables 3-1 and 3-2 were utilized to predict the nominal dynamic resolution performance of the panoramic cameras during a mission. These predictions are shown in Tables 3-3 and 3-4. The predictions were made for a 0-degree lens field angle (the center of the slit) and for three scan angles (0 degrees, 15 degrees, and 30 degrees). Since the image smear determined from the image smear budgets is a probabilistic quantity consisting of a systematic and a random component, three cases are shown in Tables 3-3 and 3-4. Case B shows the average expected performance. The expected resolution performance should fall between the upper and the lower limits established by Cases A and C respectively, with a probability of 95.5 percent. In Tables 3-3 and 3-4, the ground resolved distance, which is the geometric equivalent of the dynamic resolution, has also been entered. It should be emphasized that this quantity bears no relationship to sizes of actual objects on the ground. It only implies that the smallest resolvable tri-bar resolution target (of the right contrast) deployed on the ground would have a bar width equal to 1/2 the GRD number.

It should also be noted that the predictions do not take into account the actual degrading effects of the atmosphere on specific targets. However, the loss in contrast due to the atmosphere is anticipated and taken into account in a gross manner by making predictions for low contrast (2:1) tri-bar targets.

The dynamic resolution was computed from the static lens-film resolution (see page 3-2) and the image smear (Tables 3-1 and 3-2) utilizing the following equation

$$\frac{1}{R_d^2} = \frac{1}{R_o^2} + b^2 \tag{3.1}$$

where R_d = dynamic resolution
 R_o = static resolution
b = image smear

Equation (3.1) has no physical significance, but is an approximate way of determining the dynamic resolution when the only information available is the image smear and the static resolution. A more accurate technique based on experimental data is described in Section 4.1.

3.3 PREDICTED PERFORMANCE FROM LABORATORY DATA

Dynamic resolution tests were performed in the laboratory on all systems as part of the normal acceptance procedures. The low contrast (2:1) resolution values obtained at peak focus are shown in Table 3-5 for systems 1101 through 1105. In the same table, the corresponding GRD numbers have been entered.



~~TOP SECRET~~

~~CORONA TALENT KEYHOLE NOFORN~~



Table 3-1 — Cross-Track Image Smear Budget, 2.44-Millisecond Exposure, 3σ Values, 3404 Film

Source	Error Type	Image Smear, microns		Accuracies Assumed
		80 nm	100 nm	
Camera				
Vibration	R*	2.0	1.0	
Film lift	S†	1.78	1.42	.0007-inch film lift
Lens distortion	S	0.83	0.64	5-micron distortion at edge of format
Nodal point location	F‡	0.44	0.36	± 0.002 inch
Cross-track image motion	S	9.8 sin 2θ¶	7.9 sin 2θ	
Interface				
Yaw alignment	F	0.24 cos ² θ	0.19 cos ² θ	11 minutes
Pitch alignment	F	0.11 sin 2θ	0.086 sin 2θ	11 minutes
Vehicle				
Roll attitude	R	0.17 sin ² θ	0.13 sin ² θ	0.54 degree
Yaw attitude	R	1.11 cos ² θ	0.89 cos ² θ	0.84 degree
Yaw programmer	R	1.29 cos ² θ	1.06 cos ² θ	1 degree
Pitch attitude	R	0.42 sin 2θ	0.33 sin 2θ	0.70 degree
Roll rate	R	0.12	0.12	18 degrees per hour

* Random errors.

† Systematic error.

‡ Systematic error varying between cameras.

¶ θ = scan angle.

~~TOP SECRET~~

~~CORONA TALENT KEYHOLE NOFORN~~



Handle Via

~~TALENT KEYHOLE~~

Control Systems Jointly



Table 3-2 — Along-Track Image Smear Budget, 2.44-Millisecond
Exposure, 3σ Values, 3404 Film

Source	Error Type	Image Smear, microns		Accuracies Assumed
		80 nm	100 nm	
Camera				
Vibration	R	2.0	1.2	
IMC servo	R	$2.23 \cos \theta$	$1.78 \cos \theta$	3 percent
IMC cam error	R	$2.23 \cos \theta$	$1.78 \cos \theta$	3 percent
Uncompensated image motion	S	1.85	1.48	At edge of format
Interface				
Orbital determination	R	$2.23 \cos \theta$	$1.78 \cos \theta$	3 percent
V/h command	R	$2.23 \cos \theta$	$1.78 \cos \theta$	3 percent
Roll alignment	F	$0.24 \sin \theta$	$0.19 \sin \theta$	11.4 minutes
Pitch alignment	F	$0.120 \cos \theta$	$0.095 \cos \theta$	11 minutes
Vehicle				
Roll attitude	R	$0.68 \sin \theta$	$0.54 \sin \theta$	0.54 degree
Pitch attitude	R	$0.47 \cos \theta$	$0.37 \cos \theta$	0.70 degree
Pitch rate	R	$0.10 \cos \theta$	$0.10 \cos \theta$	14.4 degrees per hour
Yaw rate	R	$0.10 \sin \theta$	$0.10 \sin \theta$	14.4 degrees per hour
Terrain height variation	R	0.36	0.29	3,000 feet



Table 3-3 — Predicted System Performance, 80 nm, 2 σ Values,
0-Degree Field, 2:1 Contrast, 2.44-Millisecond Exposure,
3404 Film, II Generation Lens With Wratten No. 21 Filter

Case	Along Track			Cross Track		
A. 2σ Best						
Format position, degrees	0	15	30	0	15	30
Image smear, microns	0.1	0.1	0.1	0.2	3.2	6.9
Resolution, lines per millimeter	140	140	140	140	128	101
GRD, feet	6.1	6.3	7.1	5.9	6.9	10.9
B. Average						
Format position, degrees	0	15	30	0	15	30
Image smear, microns	1.1	1.1	1.0	1.8	4.9	8.5
Resolution, lines per millimeter	138	138	139	136	115	90
GRD, feet	6.2	6.4	7.1	6.1	7.7	12.2
C. 2σ Low						
Format position, degrees	0	15	30	0	15	30
Image smear, microns	3.3	3.2	2.9	3.6	6.6	10.1
Resolution, lines per millimeter	127	128	130	125	103	81
GRD, feet	6.7	6.9	7.6	6.6	8.6	13.6



~~TOP SECRET~~

~~CORONA TALENT KEYHOLE NOFORN~~



Table 3-4 — Predicted System Performance, 80 nm, 2σ Values,
0-Degree Field, 2:1 Contrast, 3.64-Millisecond Exposure,
3404 Film, III Generation Lens With Wratten No. 25 Filter

Case	Along Track			Cross Track		
A. 2σ Best						
Format position, degrees	0	15	30	0	15	30
Image smear, microns	0.1	0.1	0.1	0.3	4.8	10.3
Resolution, lines per millimeter	180	180	180	180	136	85
GRD, feet	4.8	4.9	5.5	4.6	6.5	13.0
B. Average						
Format position, degrees	0	15	30	0	15	30
Image smear, microns	1.6	1.6	1.5	2.7	7.3	12.7
Resolution, lines per millimeter	173	173	174	162	109	72
GRD, feet	5.0	5.1	5.7	5.1	8.1	15.3
C. 2σ Low						
Format position, degrees	0	15	30	0	15	30
Image smear, microns	4.9	4.8	4.3	5.4	9.8	15.0
Resolution, lines per millimeter	135	136	142	129	89	63
GRD, feet	6.3	6.5	7.0	6.4	10.0	17.5

~~TOP SECRET~~

~~CORONA TALENT KEYHOLE NOFORN~~



Handle Via

~~TALENT KEYHOLE~~

Control Systems Jointly



Table 3-5 — Laboratory Resolution Tests at Center of Format
(resolution from laboratory data, GRD obtained
from resolution for 80 nm)

System	FWD				AFT			
	Along Track		Cross Track		Along Track		Cross Track	
	Resolution, lines per millimeter	GRD, feet	Resolution, lines per millimeter	GRD, feet	Resolution, lines per millimeter	GRD, feet	Resolution, lines per millimeter	GRD, feet
System 1101								
Best	143	6.0	128	6.5	143	6.0	128	6.5
Mean	125	6.9	119	6.9	128	6.7	122	6.8
Low	101	8.5	114	7.3	114	7.5	114	7.3
System 1102								
Best	143	6.0	143	5.8	128	6.7	128	6.5
Mean	134	6.4	140	5.9	123	7.0	120	6.9
Low	128	6.7	128	6.5	114	7.5	114	7.3
System 1103								
Best	143	6.0	160	5.2	143	6.0	143	5.8
Mean	143	6.0	150	5.5	137	6.3	134	6.2
Low	143	6.0	143	5.8	128	6.7	128	6.5
System 1104								
Best	180	4.8	180	4.6	160	5.4	143	5.8
Mean	176	4.9	168	4.9	143	6.0	140	5.9
Low	160	5.4	160	5.2	128	6.7	128	6.5
System 1105								
Best	202	4.2	202	4.1	180	4.8	160	5.2
Mean	188	4.6	186	4.4	158	5.4	158	5.2
Low	180	4.8	180	4.6	151	5.7	151	5.5



4. DETERMINATION OF MISSION RESOLUTION

4.1 DESCRIPTION OF TECHNIQUE

One of the major accomplishments of this study was the development of a technique for predicting the dynamic resolution and the corresponding ground resolved distance for any point on the panoramic format and any frame photographed during a mission provided, of course, that the required data were available. This technique has been very useful in the performance evaluation of systems 1101 through 1104. It provides the data needed to evaluate the systems and gives insight into the factors affecting the performance of individual systems. The basic concept of the technique is described below.

1. A specific point on a given frame is identified.
2. The image smear and the static lens-film resolution are determined for that point.
3. The image smear and the static resolution are combined in a formula to produce the dynamic resolution.
4. The ground resolved distance is computed from the dynamic resolution utilizing the appropriate geometric relationships.

4.1.1 Static Resolution

Individual targets for which the dynamic resolution and GRD are to be computed are identified by pass number, frame number, and x, y coordinates according to the universal grid system. In order to determine the static resolution at a point of interest, the static resolution versus focus position tests that have been performed on the respective Petzval lenses are utilized. These tests are performed by the contractor's optics division upon final assembly of the lens optical elements and before a lens is assembled on a panoramic camera. The tests are performed on a Mann optical bench using a parabolic collimator, high contrast and low contrast (2:1) tri-bar resolution targets, 3404 film, and the primary filters (Wratten no. 21 for II generation lenses, and Wratten no. 25 for III generation lenses). The angular field of the Petzval is essentially one dimensional (in the y or along-track direction of the panoramic format). The total angular field of the lens is approximately 6 degrees (± 3 degrees from the center).* During these static resolution tests, the focal position occupied by the film samples is varied in increments of 0.001 inch, and the film-lens resolution is determined at seven positions across the lens angular field (every 1 degree, i.e., 0, ± 1 , ± 2 and ± 3 degrees). The data obtained from these tests is (approximately) the static lens-film resolution as a two-dimensional function of field angle and focus position. The static resolution of any point on the panoramic format can be obtained from this two-dimensional function

* The along-track angular field of the panoramic camera is smaller (approximately 5 degrees).

~~TOP SECRET~~

~~CORONA TALENT-KEYHOLE NOFORN~~

if the field angle and focus position it occupies are known. The field angle of a point can be determined from its y coordinate by the equation

$$\beta = \tan^{-1}\left(\frac{y - y_0}{f}\right) \quad (4.1)$$

where β = field angle

y_0 = 2.8 centimeters (y coordinate for a 0-degree field angle)

f = lens focal length (24 inches)

In order to determine the focus position of a point, more information is needed. In the laboratory, a dynamic film flatness test is performed on each panoramic camera. The results of this test are samples over the panoramic format of the amount of dynamic film lift above the focal plane rollers (in units of 10^{-3} inch). The dynamic film lift at the point of interest can be determined from this data by utilizing the x, y coordinates of the point. Actually, the information which is essential is not the absolute value of film lift at the point of interest, but the relative film lift with respect to the film lift at the center of the format (x = 37.8 centimeters, y = 2.8 centimeters). From the film flatness tests, therefore, one can determine the relative focus position of a point on the panoramic format with respect to the center of the format. Finally, the focus position occupied by the film at the center of the format can be deduced from the final dynamic resolution versus focus position tests performed on every panoramic camera. These resolution tests provide the absolute focus position at the center of the format. Hence, the absolute focus position for a specific point is obtained from the absolute focus position of the center of format and the relative focus position of the point with respect to the center of format.

4.1.2 Computation of Image Smear

Image smear results because during the exposure of a panoramic format, the images of ground targets have a velocity relative to the film. This velocity can be separated into two orthogonal components, one component in the along-track direction which affects the along-track resolution and the other in the cross-track direction affecting the cross-track resolution. The total image smear in either direction is directly proportional to the exposure time. This is an assumption strictly true only for linear image smear (image smear velocity being constant during the exposure time). For example, image smear resulting from vibration is not strictly linear. However, due to the short exposure times (less than 5 milliseconds) compared with the time constants of the entire photographic system (panoramic cameras and vehicle), the image smear is expected to be approximately linear.

In general, the total image smear in either direction displays significant variations over the panoramic format. The major sources of image smear appear in the error budgets (Tables 3-1 and 3-2). The total image smear also varies with the altitude of the vehicle. The low altitudes produce larger image smears than the high altitudes. This is due mainly to the higher V/h rates and the faster operation of the panoramic cameras at low altitudes.

The image smear in either direction is being computed utilizing equations similar to the error budgets. Since there are not enough data to compute all the image smear components exactly, the image smear consists of a systematic value, b_s , and a random one, b_r . The algebraic sum of all the components whose values and signs (plus or minus) can be established from the available flight data is b_s . On the other hand, b_r is the root sum square of all the random components and all the components whose sign is unknown. For each random component, a root mean square value

~~TOP SECRET~~

~~CORONA TALENT-KEYHOLE NOFORN~~

Handle Via

~~TALENT-KEYHOLE~~

Control Systems Jointly

~~TOP SECRET~~

~~CORONA TALENT KEYHOLE NOFORN~~

was entered. After b_r and b_s have been computed, the total image smear in either direction, b_t , is obtained by adding the magnitudes of b_r and b_t . In other words,

$$b_t = b_r + |b_s| \quad (4.2)$$

In Equation (4.2), b_t becomes a probabilistic quantity. If we assume that b_r is the root mean square value of a Gaussian random variable, then Equation (4.2) means that the probability of the actual image smear being smaller than b_t is between 68 and 84 percent. (If $|b_s| = 0$, the probability is 68 percent, and if $|b_s|$ is much greater than b_r , the probability is almost 84 percent.) Obviously, the most accurate determination of the total image smear results when b_r is much smaller than $|b_s|$. When b_t is computed, the following data are utilized from the mission ephemeris:

1. Vehicle altitude
2. Vehicle ground track velocity
3. Panoramic camera scanning rate
4. Panoramic camera slit width
5. Programmed vehicle yaw angle
6. Required vehicle yaw angle from orbital mechanics.

Additional laboratory data used in the computation of b_t are:

1. Camera cam constant. (The ratio between FMC and scanning rates during format exposure, nominally 0.01321.)
2. Along-track camera image smear.
3. Cross-track camera image smear. This image motion component has a direction opposite to the direction at which the focal plane rollers scan the panoramic format.

The exposure time is related to the slit width and scanning rate by the following formula:

$$TE = \frac{SLIT}{(SCR) f} \quad (4.3)$$

where TE = exposure time
SLIT = slit width
SCR = scanning rate
f = focal length

Also, the FMC rate and scanning rate are related by Equation (4.4).

$$FMC = (CAM) SCR \quad (4.4)$$

where FMC = FMC rate
CAM = cam constant discussed above

~~TOP SECRET~~

~~CORONA TALENT KEYHOLE NOFORN~~

Handle Via

~~TALENT KEYHOLE~~

Control Systems Jointly

~~TOP SECRET~~

~~CORONA TALENT-KEYHOLE NOFORN~~



4.1.3 Computation of Dynamic Resolution

In order to determine the dynamic resolution at a point of interest on the panoramic format, the static resolution and image smear are combined into a formula. The formula that has been used very often is the following:

$$\frac{1}{R_d^2} = \frac{1}{R_s^2} + b^2 \quad (4.5)$$

where R_d = dynamic resolution
 R_s = static resolution
 b = image smear

There is no physical justification for this formula and at best it is only a very rough approximation. On the other hand, it is possible to establish the relationship between R_d , R_s , and b experimentally. This relationship can be obtained by performing, in the laboratory, dynamic resolution tests on the corresponding panoramic camera. During these resolution tests, known amounts of image smear are selectively introduced by mismatching the target wheel speed to the FMC rate of the camera. The result of these tests is an experimental curve of dynamic resolution versus image smear. It was found that this experimental curve can be described by the following expression:

$$R_d = \frac{R_s}{[1 + (bR_s)E_1]^{E_2}} \quad (4.6)$$

The exponents E_1 and E_2 can be selected such that Equation (4.6) is a good approximation of the experimental curve well within the error of plotting the experimental curve. Note that Equation (4.6) reduces to Equation (4.5) by setting $E_1 = 2$ and $E_2 = 1/2$. Exponents E_1 and E_2 were found to vary between various Petzval lenses, and for a given lens they vary depending on the focus position occupied by the film.

When E_1 and E_2 have been determined for a given lens, the dynamic resolution, R_d , can be determined from the static resolution, R_s , and the image smear, b , from Equation (4.2), by utilizing Equation (4.6).

Finally, the ground resolved distance is determined as the geometric projection on the ground of a length increment on the film, which is the inverse of the dynamic resolution.

Dynamic resolution and ground resolved distance predictions were computed for the CORN target images and HPL or first priority target images. These predictions have been presented in Appendices A and B of the performance evaluation reports for Missions 1101 through 1104. The computations required for the predictions were carried out in a computer. However, the static resolution values which were essential to the predictions were determined manually.

4.2 EVALUATION OF TECHNIQUE

4.2.1 Main Advantage of Technique

The contractor feels that the method of predicting the dynamic resolution which was described in Section 4.1 has been very successful, mainly because it utilizes most of the available laboratory data which in turn supply much a priori information about the panoramic cameras. From one point

~~TOP SECRET~~

~~CORONA TALENT-KEYHOLE NOFORN~~

Handle Via
~~TOP SECRET~~
Control Systems Jointly

~~TOP SECRET~~

~~CORONA TALENT-KEYHOLE NOFORN~~

of view, this technique may be compared with a neat trick, because the dynamic resolution is not being predicted from "scratch." On the contrary, the dynamic resolution is obtained from the static resolution by modifying it for the predicted amount of image smear. The strength of the method arises from the fact that the static resolution is being measured in the laboratory under controlled experimental conditions and can be determined very accurately. Furthermore, the relationship between dynamic resolution and image smear can be accurately established in the laboratory. Hence, if the static resolution, R_s , and the exponents, E_1 and E_2 , are known accurately, a large percentage error in the computation of image smear will produce a much smaller percentage error in the prediction of dynamic resolution. In other words, the accuracy of the dynamic resolution depends mainly on the accuracy of the static resolution.

4.2.2 Significant Errors

The accuracy of the resolution predictions is affected by various errors throughout the data which are utilized by the prediction method. However, the major contributors of error are the following:

1. Accuracy of static resolution data
2. Environmental focus shifts
3. Unknown cross-track image smear.

The experimental error associated with the determination of resolution in the laboratory was found to be significant. This is due mainly to the statistical nature of resolution. For the Petzval lenses and 3404 film, the experimental error increases rapidly for resolution values larger than 100 lines per millimeter. A special static resolution test was performed to determine the statistics of the experimental error. The lens was a third generation Petzval with a Wratten no. 25 filter; the film was SO-380 (3404 emulsion on ultrathin base). The average low-contrast resolution was approximately 165 lines per millimeter, and the rms value of the experimental error for a single resolution reading was approximately 20 lines per millimeter. In order to improve the accuracy of the resolution data, it is necessary to obtain many resolution samples (readings) and average them. Evaluation of the statistics obtained from this test showed that the average of 5 resolution readings would have an rms error of 9 lines per millimeter, while the average of 10 readings would have an rms error of 6.5 lines per millimeter. However, if one averaged 5 readings out of 10 available readings by eliminating the highest reading and the four lowest readings, the rms error of this average should be approximately 4 lines per millimeter.

The environmental focus shifts are discussed in detail in Section 5.6. If these focus shifts are not known, they may produce some gross errors in the static resolution values. Fortunately, the deployment of CORN targets allows one to determine these focus shifts to a large extent, but the remaining errors in the focus position occupied by the film result in static resolution errors which may or may not be significant, depending on the portion of the resolution versus focus curve on which the film is located. Other possible errors in the static resolution values could result from differences between the laboratory film flatness data and the actual flatness characteristics of the film during a mission. There is no information available about all the effects of the mission environment on the flatness characteristics. In addition, some random variation of the flatness characteristics should be expected from one frame to another, while the laboratory flatness data describe only the systematic characteristics.

A residual image smear velocity exists in the cross-track direction which results from the scanning motion of the focal plane rollers. This type of image smear velocity is a characteristic of all panoramic cameras regardless of design. This image smear velocity has been compensated

~~TOP SECRET~~

~~CORONA TALENT-KEYHOLE NOFORN~~

Handle Via

~~TALENT-KEYHOLE~~

Control Systems Jointly

~~TOP SECRET~~

~~CORONA TALENT KEYHOLE NOFORN~~

to some extent by offsetting the lens from its rear node, but it has not been entirely eliminated because it varies in magnitude over the length of the format. This image smear velocity has been measured in one camera, and the information obtained has been incorporated in the computer program for predicting dynamic resolution and GRD. It is possible that other cameras may have similar image smear velocities but they may be different enough to produce errors in the computation of the cross-track image smear. In any case, the probability of a significant error in the cross-track image smear is expected to be very small except for long exposure times.

4.2.3 Comparison of CORN Target and Predicted Resolutions

Tables 4-1 through 4-6 have been prepared as a means of comparing the GRD predictions with readings obtained from the corresponding mission films. A direct comparison between the predictions and the readings is not possible because the predictions were made for targets of 2:1 contrast (0.333 modulation), while the apparent contrast of the CORN and fixed targets varies and is affected by weather conditions.

One of the degrading effects of the atmosphere is reduction of contrast of ground objects (see Section 5.8). The CORN (mobile) targets have a nominal contrast of 4.7:1. However, their apparent contrast, as seen through the atmosphere, varies significantly about a contrast of 2:1 depending on weather conditions. Hence, the main limitation of the resolution prediction technique is its inability to account for the atmospheric effects on the system performance. In order to eliminate this limitation, it would be necessary to alter the technique drastically and some of its advantages (the technique is based on experimental data) would be lost. Furthermore, even if the technique could be altered or a new accurate technique could be developed, additional data about the loss of contrast due to the atmosphere must be provided for all targets for which resolution predictions are to be made. These data are not available at the present time. It seems that the Crystal Ball* program could provide this contrast loss information (contrast factor) if the haze conditions over a target could be specified.

Another difficulty with the CORN targets is the fact that for GRD values larger than 8 feet, there are only two panels (one for 12-foot GRD and one for 16-foot GRD). Thus, the maximum quantization error for GRD values larger than 8 feet is +4, -0 feet. Had the CORN target been a $\sqrt{2}$ target for GRD values larger than 8 feet, there would have been five panels between the 8-foot GRD and the 16-foot GRD panels instead of only one panel.

Another point that should be emphasized is that resolution and GRD are fairly inexact quantities. A study conducted by the contractor showed that wide variations in readings exist for deployed targets photographed in missions 1101 through 1103. (A reading is a GRD determination by one person from a given target image.) The sources of the readings for this study were two government agencies and the contractor. Readings for the same target image varied usually two or three elements. An element is a 12 percent change in GRD for values less than 8 feet and 50 percent for GRD values larger than 8 feet. The statistics of the readings per mission are presented on the following page.

* PAR 24-8-85 Final Report, Study the Characteristics and Uses of Suitable Materials for High Altitude Acquisition (████████████████████ 14 October 1968).

~~TOP SECRET~~

~~CORONA TALENT KEYHOLE NOFORN~~

Handle Via

~~TALENT KEYHOLE~~

Control Systems Jointly

~~TOP SECRET~~

~~CORONA TALENT KEYHOLE NOFORN~~



Mission	Unanimous Agreement, percent	2-Element Spread, percent	3-Element Spread, percent	4-Element Spread, percent
1101	10	45	40	5
1102	31	54	15	0
1103	14	43	36	7

Taking all three missions together as a whole:

Unanimous Agreement, percent	2-Element Spread, percent	3-Element Spread, percent	4-Element Spread, percent
17	47	32	4

This study points out that high accuracies should not be expected from the readings or any type of resolution predictions because of the statistical nature of resolution.

The contractor estimates that the accuracy of the resolution prediction method is between 10 and 20 percent.

~~TOP SECRET~~

~~CORONA TALENT KEYHOLE NOFORN~~



Handle Via

~~TALENT KEYHOLE~~

Control Systems Jointly



Table 4-1 — CORN Target Resolution, Comparison of Readings and Predictions, Mission 1101, FWD-Looking Camera, Low Contrast (2:1)

Pass	Frame	Along Track			Cross Track		
		Modulation	Actual Resolution, lines per millimeter	Predicted Resolution, lines per millimeter	Modulation	Actual Resolution, lines per millimeter	Predicted (Low Contrast) Resolution, lines per millimeter
14	13	0.427	16	16.3	0.403	>16	18.1
14	31	-	8-12	11.5	0.422	8-12	11.7
111	22	-	12-16*	12.0	0.190	>16*	9.8
127	15	-	10.8*	12.1	-	>16*	11.3
127	23	0.278	8-12	9.0	0.315	12-16	9.1
143	20	0.357	8-12	-	0.344	12-16	-
157	9	0.427	7.12-8	13.7	0.408	8.12	9.7
173	19	0.457	8-12	-	0.446	12	-

*From dupe positive readings.



Table 4-2 -- CORN Target Resolution GRD, Comparison of Readings and Predictions,
Mission 1101, AFT-Looking Camera

Pass	Frame	Along Track			Cross Track		
		Modulation	Actual Reading, feet	Predicted Low Contrast, feet	Modulation	Actual Reading, feet	Predicted Low Contrast, feet
14	19	0.422	>16	16.6	0.385	>16	17.1
14	37	-	>16	14.0	0.315	12-16	14.6
111	28	-	>16*	18.7	0.329	>16*	17.5
127	19	-	13.8*	16.7	-	>16*	15.7
127	29	0.315	>16	13.3	0.329	>16	13.6
143	26	0.365	>16	19.2	0.375	>16	21.6
157	16	0.457	>16	17.8	0.422	16	16.1
173	25	0.417	>16	-	0.474	>16	-

*From dupe positive readings.

~~TOP SECRET~~

~~CORONA TALENT KEYHOLE NOFORN~~



Table 4-3 — CORN Target Readings and Predictions, Mission 1102, FWD-Looking Camera

Pass	Frame	Along Track			Cross Track			Weather	Contrast	Target Type
		Average Reading, feet	Modulation	Predicted GRD, feet	Average Reading, feet	Modulation	Predicted GRD, feet			
16	6	7.7	-	10.0	7.9	-	7.5	Clear	Fair	Fixed, medium contrast
32	13	8	-	7.4	8-12	-	7.0	Clear	Fair	CORN
48	21	8-12	0.061	7.6	12-16	0.061	6.4	Cloudy	Low	CORN
48	48	6.9	-	8.3	6.5	-	7.4	Clear	Good	Fixed
97	15	8-12	-	10.3	12-16	-	14.7	Clear	Fair	CORN
113	24	13*	-	10.7	25*	-	24.6	Slight haze	Poor	Fixed
176	26	11*	-	8.3	>16*	-	6.4	Heavy haze, cloudy	Poor	Fixed

*Dupe positive readings only.

~~TOP SECRET~~

~~CORONA TALENT KEYHOLE NOFORN~~



Handle Via

~~TALENT KEYHOLE~~

Control Systems Jointly



Table 4-4 — CORN Target Readings and Predictions, Mission 1102, AFT-Looking Camera

Pass	Frame	Along Track				Cross Track			Weather	Contrast	Target Type
		Average Reading, feet	Modulation	Predicted GRD, feet	Average Reading, feet	Modulation	Predicted GRD, feet				
16	12	9	-	9.0	9	-	7.7	Clear	Fair	Fixed, medium contrast	
32	19	8-12	-	7.3	8-12	-	7.3	Clear	Fair	CORN	
48	54	8.0	-	8.8	7.2	-	8.4	Clear	Good	Fixed	
97	21	13.3	0.239	9.8	12-16	0.239	11.9	Clear	Fair	CORN	
176	32	10.5*	-	8.2	>16*	-	8.0	Cloudy, heavy haze	Poor	Fixed	

*Dupe positive readings only.

~~TOP SECRET~~

~~CORONA TALENT-KEYHOLE NOFORN~~



Table 4-5 — CORN Target Readings and Predictions,* Mission 1103

AFT-Looking Camera

Pass	Frame	Along Track		Cross Track		Apparent Contrast
		Average Reading, feet	Predicted GRD, feet	Average Reading, feet	Predicted GRD, feet	
16	13	9	7.8	9	7.1	<2:1
16	21	12-16	7.7	12-16	7.7	1.36:1
97	13	10	6.9	8	7.5	1.89:1
97	20	7.5	7.1	8-12	7.9	2.05:1

FWD-Looking Camera

16	7	9	8.6	8	6.9	1.73:1
97	7	7.5	7.0	8-12	7.2	1.73:1

* Predictions are for low contrast (2:1) targets.

~~TOP SECRET~~

~~CORONA TALENT-KEYHOLE NOFORN~~



Handle Via

~~TALENT-KEYHOLE~~

Control Systems Jointly

~~TOP SECRET~~

~~CORONA TALENT KEYHOLE NOFORN~~



Table 4-6 — CORN Target Readings and Predictions, * Mission 1104

FWD-Looking Camera

Pass	Frame	Along Track		Cross Track	
		Average Reading, feet	Predicted GRD, feet	Average Reading, feet	Predicted GRD, feet
14	6	8.0	7.3	7.1	6.9
16	6	5.7	5.9	8.0	6.1
129	10	6.1	6.0	6.8	5.7
129	12	5.5	6.3	6.8	8.2
129	13	4.8	7.1	6.8	7.8
145	32	8.0	6.4	7.0	7.0

AFT-Looking Camera

14	12	8.0	7.8	8.0	7.7
16	6	8.0	7.7	8.0	6.7
145	38	8.0	6.8	8.0	6.4

* Predictions applicable to targets of 2:1 contrast.

~~TOP SECRET~~

~~CORONA TALENT KEYHOLE NOFORN~~



Handle Via

~~TALENT KEYHOLE~~

Control Systems Jointly

~~TOP SECRET~~

~~CORONA TALENT-KEYHOLE-NOFORN~~



5. SYSTEM EVALUATION

5.1 ALTITUDE OF PHOTOGRAPHY

The altitude of photography is one of the most important factors determining the ability of a photographic system to gather intelligence. A 10 percent change in altitude is considered to have a significant effect on the small detail of ground targets. Reducing the altitude of photography is a better way to improve the intelligence-gathering performance of the system than increasing the focal length and/or the dynamic camera resolution (all other parameters being equal, i.e., coverage).

The average altitude of photography for first priority targets is approximately 88 nm. These targets have an average latitude of 50 °N (approximately). In addition, the perigee is located farther south and has the tendency to move northward as the mission progresses. The first priority targets could be photographed from an altitude of 80 nm if the perigee could be maintained at 50 °N latitude with a perigee altitude of 80 nm. A 10 percent increase in the scale of the photography could be achieved by controlling the orbit in this fashion.

5.2 V/h PROGRAMMING ERRORS

V/h programming errors affect the FMC rate of the panoramic cameras and result in image smear in the along-track direction. The amount of image smear is linearly related to the V/h error and the exposure time. To determine if an FMC rate error exists, one multiplies the scanning rate of the camera by the cam constant and then compares it with the V/h rate. (These data are taken from the mission ephemeris.) This FMC rate error is a constant or very slowly varying error. Variations in the scanning rate occurring within a camera cycle will not be detected since the scanning rate is determined by the time interval between successive center of format switch activations. This switch closes once per camera lens revolution. The resulting FMC rate error may be due to V/h programming errors or to camera errors. However, when the FMC rate error is identical for both cameras of the stereo pair and it varies throughout the mission, the probability that it is due to programming errors rather than camera errors is overwhelming. Such V/h programming errors have been evaluated for missions 1102, 1103, and 1104 and for frames that contained either CORN targets or first priority targets. The results are shown in Table 5-1 where the V/h programming error is expressed as a percentage of the correct FMC rate. Table 5-1 shows that the rms error has been reduced and for mission 1104 it can be considered negligible.

5.3 CAMERA SMEAR SOURCES

There are two significant sources of image smear which can be attributed to the panoramic camera construction and operation. In the cross-track direction, a residual image smear velocity exists which results from the scanning motion of the focal plane rollers over the film (see also Section 4.2.2). This image smear velocity is added algebraically to the uncompensated cross-track image motion predicted by the error budgets and mentioned also in Section 2.2. The uncompensated

~~TOP SECRET~~

~~CORONA TALENT-KEYHOLE-NOFORN~~

~~TOP SECRET~~

Handle Via
~~TALENT-KEYHOLE~~
Control Systems Jointly



cross-track image motion is due entirely to the forward motion of the vehicle and the stereo convergence angle. The combination of these two cross-track smear velocities may produce appreciable cross-track smears at certain areas of the panoramic format, especially when the exposure time is longer than 3 milliseconds. Figs. 5-1 and 5-2 show the expected cross-track smear from these two sources computed from the corresponding equations of the resolution prediction computer program. In the laboratory, in order to partially correct the cross-track image at the center of format (0 degrees scan angle) the rear node of the lens would be displaced from the mechanical axis of rotation 0.010 to 0.020 inch. The result of this displacement is to move the curves of Figs. 5-1 and 5-2 toward negative smear values by an amount proportional to the node displacement and the slit width. (Positive image smear in Figs. 5-1 and 5-2 is defined as image motion from the supply side of the format toward the takeup side.) Both Figs. 5-1 and 5-2 include a 0.010-inch rear node displacement. The dynamic resolution of the camera in the cross-track direction is affected by the magnitude of the total image smear and is insensitive to its direction. (10 microns of image smear would limit the dynamic resolution to approximately 90 lines per millimeter.) However, the direction of an image smear component is important, since the image smear components add algebraically. It should be mentioned that Figs. 5-1 and 5-2 do not show the total smear in the cross-track direction because other smaller smear components would be present from other sources (e.g., roll rates of the vehicle). Also, Figs. 5-1 and 5-2 represent poor target illumination conditions (winter conditions) because the curves were computed for relatively long exposures.

Table 5-1 — Statistics of V/h Programming Errors

Mission	Average, percent	RMS Error, percent	Gross Errors
1102	+1.82	2.24	Pass no. 184, 36.7 percent slow
1103	+0.11	1.31	
1104	+0.14	0.68	

NOTE: The allowable rms error in the error budgets for V/h programming is 1.41 percent.

In the along-track direction, image smear exists due to a mechanical vibration in the panoramic cameras. This image smear was discovered by analysing the panoramic geometry (PG) calibration data for system 1104. (See Section 3.4 of Performance Analysis Report for System 1102 as to the method of determining this image smear.) This image smear appears as a small sinusoidal variation of the camera cam constant with a frequency of approximately 19.4 cps. It is believed, therefore, that this vibration is a propagation into the FMC cam linkages of the basic torsional frequency of the camera structure. The resulting rms variation in the cam constant is estimated to be approximately 3 percent. For the altitude and exposure time conditions specified in Fig. 5-1, the corresponding image smear in the along-track direction would have an rms value of 2.6 microns (neither a very large image smear value nor a negligible one). In order to reduce this image smear component, it would be necessary to stiffen the camera structure considerably; the result would be an increase in the camera weight.



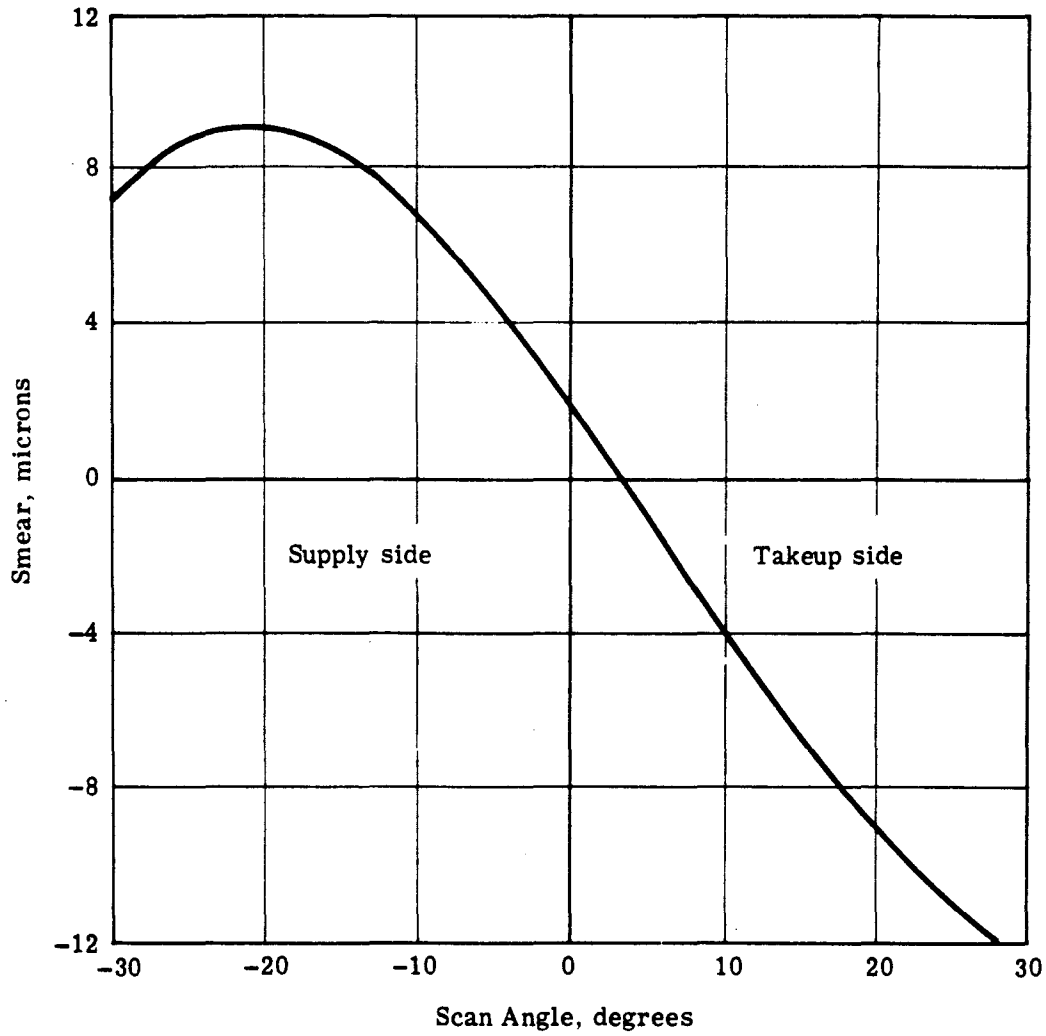


Fig. 5-1 — Cross-track smear, AFT-looking camera (altitude—85 nm, rear node offset—0.010 inch, slit width—0.270 inch, exposure—3.08 milliseconds)

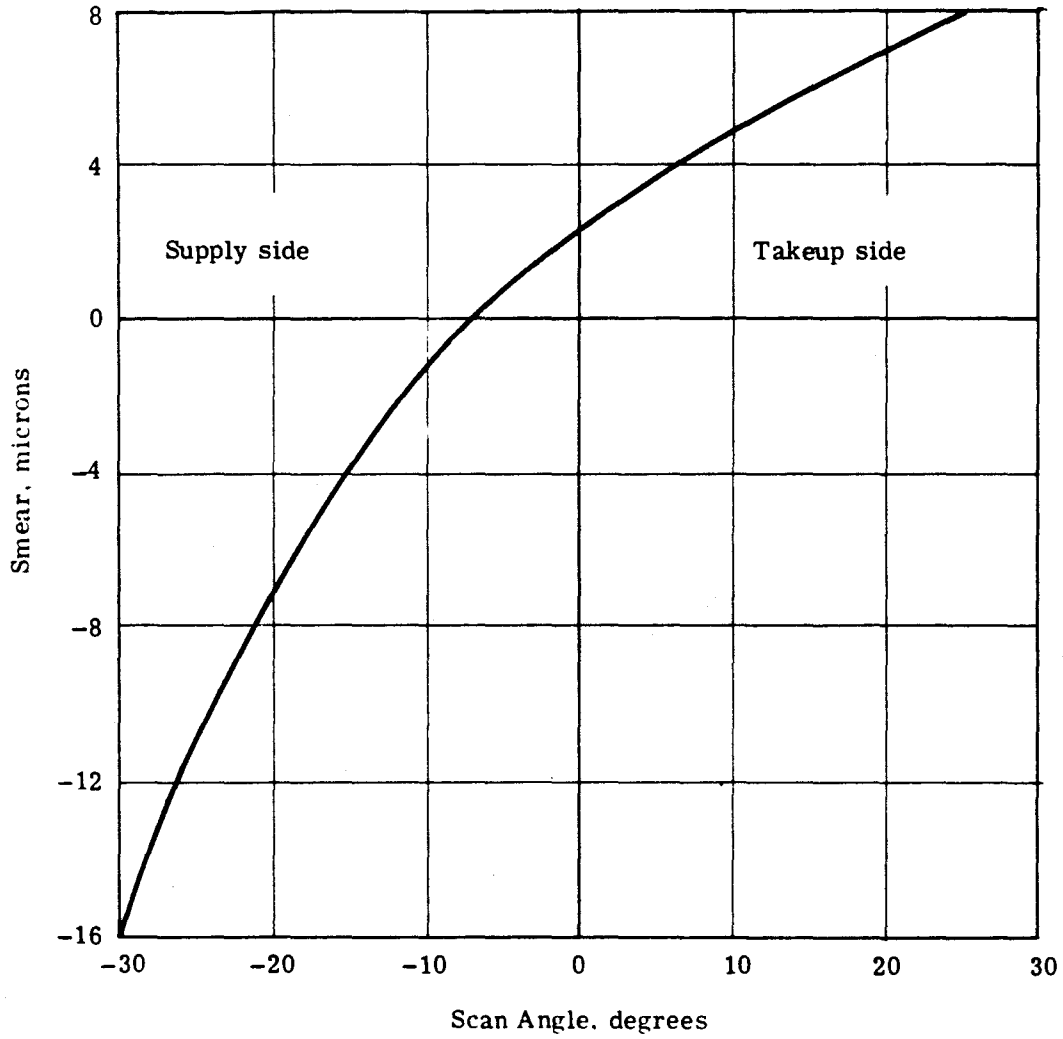


Fig. 5-2 — Cross-track smear, FWD-looking camera (altitude—85 nm, rear node offset—0.010 inch, slit width—0.340 inch, exposure—3.88 milliseconds)

~~TOP SECRET~~

~~CORONA TALENT KEYHOLE NOFORN~~

5.4 VEHICLE EFFECTS

Theoretically speaking, while the panoramic system is photographing targets on the ground, the vehicle should be absolutely stable. Its attitude rates and angles about its roll, pitch, and yaw axes should all be zero, except, of course, for the correct yaw biasing which is necessary to compensate for the correct V/h direction since the vehicle velocity combines with the rotation of the earth to produce a ground track velocity whose direction varies slightly from that of the orbit (approximately 2 degrees). In reality, of course, the stability of the vehicle is not perfect. Instead, the attitude of the vehicle is controlled within certain limits. As long as the attitude and rate errors are within these limits (included in the error budgets, Tables 3-1 and 3-2), the resulting image smears are fairly small compared with other sources of image smear. The appendix shows the effects of vehicle attitude and rate errors on image smear velocities.

The contractor has no definite attitude and rate data about any of the missions, so the effect of actual attitude and rate errors on image smear cannot be evaluated. Certain facts are known:

1. The roll axis of the vehicle is the least stable, because of the small moment of inertia about this axis. Roll rates will produce image smear in the cross-track direction adding or subtracting from the image smear described in Section 5.3.

2. The panoramic system as a unit is designed to be balanced so that a minimum of torque disturbances about any one of the three axes are transmitted to the vehicle. The cameras, the supply spools, and the takeup spools rotate in opposite directions in pairs. Hence, the system is balanced as far as possible whenever both cameras are operating synchronously (stereo operation). However, when only one camera is turned on or off, large torques (especially about the roll axis) are transmitted to the vehicle.

5.5 LENS MTF

In Section 3.1, it was mentioned that the MTF of a lens describes its performance very well. A lens is a linear spatial filter with a frequency response described by its optical transfer function (OTF) which is a complex function (amplitude and phase) of two orthogonal spatial frequency variables (e.g., one frequency variable, f_x , may be taken in the along-track direction and the other, f_y , in the cross-track direction). The amplitude of the OTF along the positive f_x axis is the MTF of the lens in the along-track direction, while the amplitude of the OTF along the positive f_y axis is its MTF in the cross-track direction. The volume under the OTF function can be considered as the capacity of the lens to transmit intelligence or information to the film. Of course, the film will not record all the information transmitted by the lens. In addition, some of the information that could be recorded is corrupted by image smear and the grain noise of the film. Fig. 5-3 shows the computed MTF's for lens I-215 (a III generation lens) and I-192 (a II generation lens) and demonstrates the improvement in quality of the III generation lens design with respect to the II generation. Assuming that the OTF is a circularly symmetric function of spatial frequency, it is estimated that the volume under the III generation lens OTF is approximately 1.4 times larger than the volume under the II generation lens OTF. Also, in Fig. 5-3, the MTF of a diffraction-limited $f/3.5$ lens has been plotted because it forms the upper limit which cannot be surpassed by further improvements in lens design (making the lens more aberration free). Fig. 5-4 shows what happens to the MTF of lens I-215 with the various filters. The loss in quality with the Wratten no. 23A filter is rather small, and this filter deserves serious consideration whenever poor illumination conditions require long exposure times if a Wratten no. 25 filter were to be used instead (see Section 5.8). The MTF of a II generation lens does not vary significantly if a Wratten no. 23A or 25 filter were to be used instead of the Wratten no. 21. Figs. 5-5 and 5-6 show the changes that occur on the MTF's as the lens focus is varied by 0.001-inch increments, and clearly demonstrate the need for the lenses to be properly focused during a mission (especially the III generation lens).

~~TOP SECRET~~

~~CORONA TALENT KEYHOLE NOFORN~~

Handle Via

5-5

~~TALENT KEYHOLE~~
Control Systems Jointly

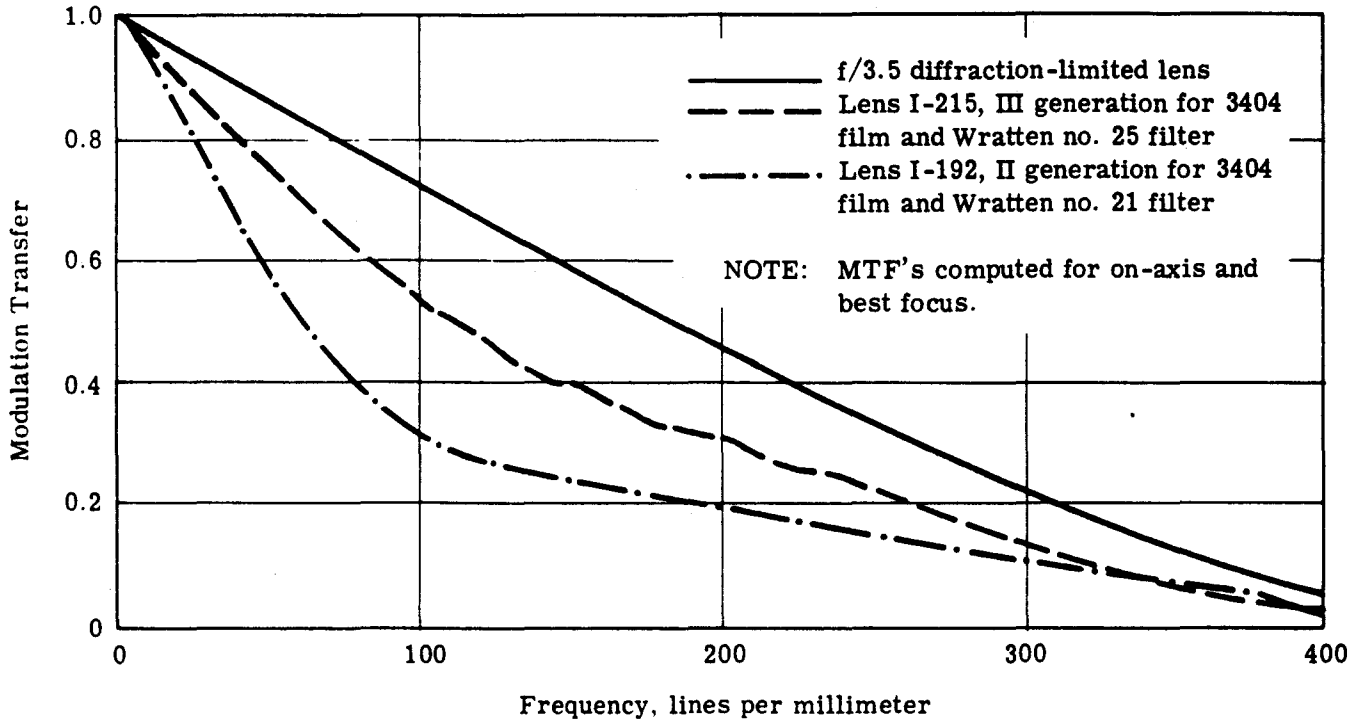


Fig. 5-3 — MTF's for lenses I-215 and I-192



~~TOP SECRET~~

~~CORONA TALENT-KEYHOLE NOFORN~~

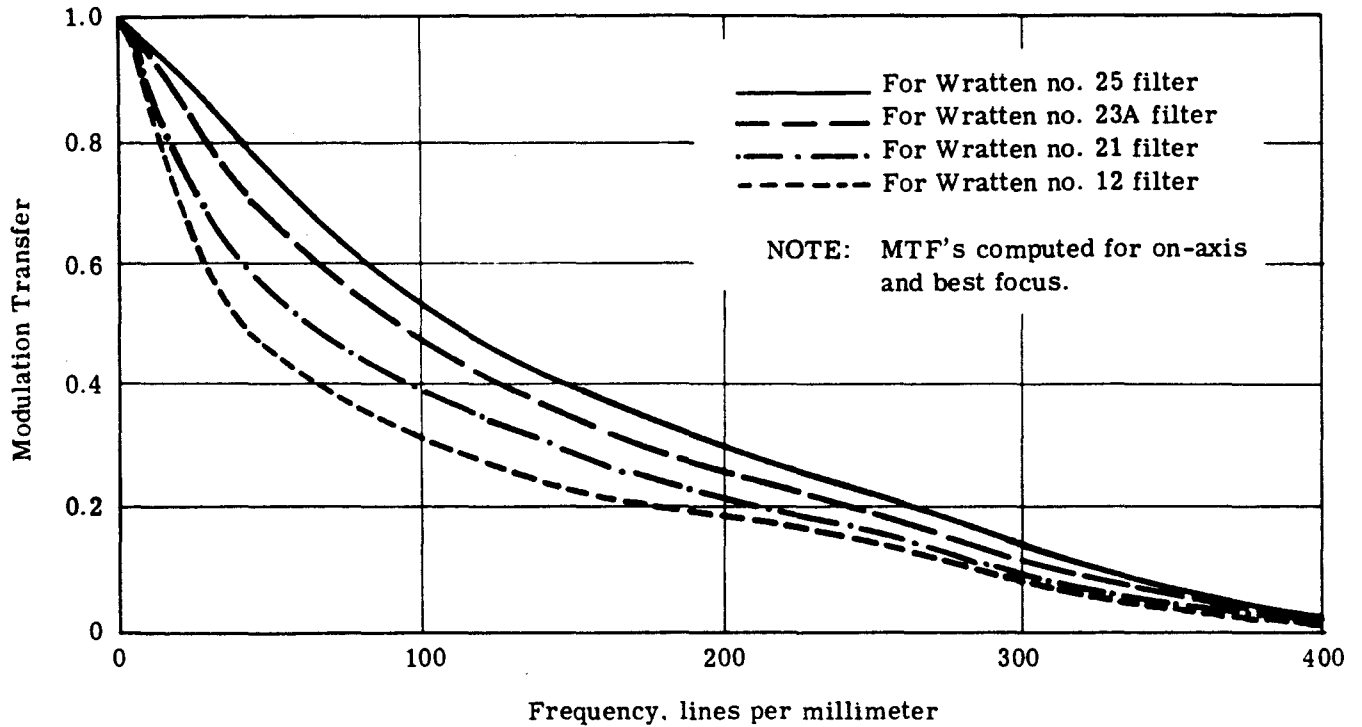


Fig. 5-4 — MTF's of lens I-215, III generation lens with 3404 film

~~TOP SECRET~~

~~CORONA TALENT-KEYHOLE NOFORN~~



Handle Via
~~TALENT-KEYHOLE~~

Control Systems Jointly

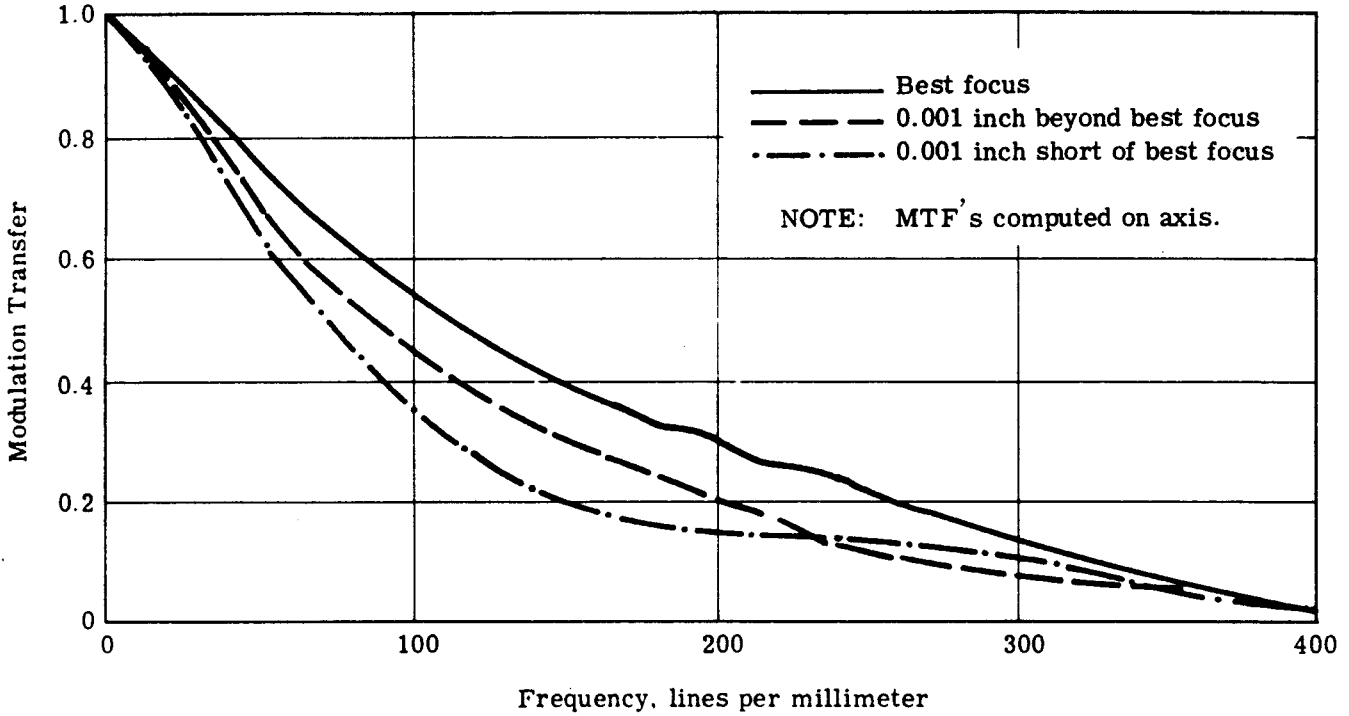


Fig. 5-5 — MTF's of lens I-215, III generation lens with 3404 film and Wratten no. 25 filter



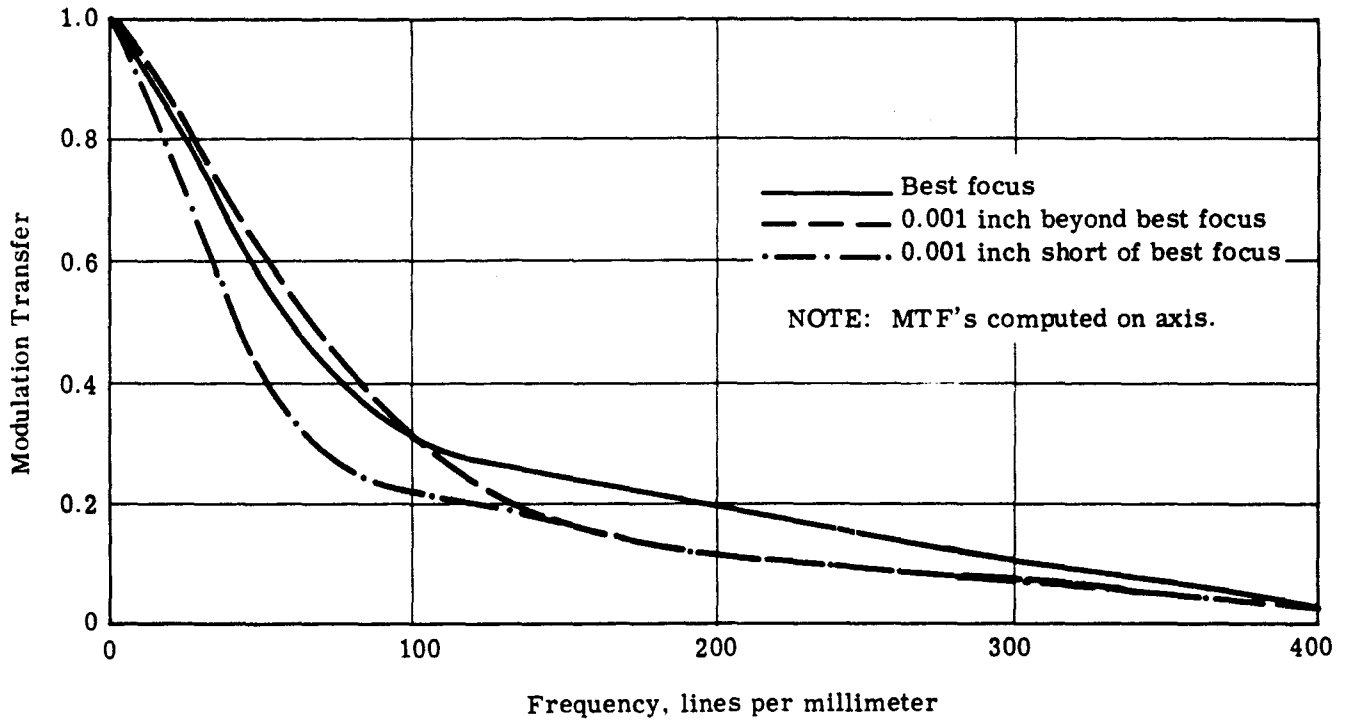


Fig. 5-6 — MTF's of lens I-192, II generation lens with 3404 film and Wratten no. 21 filter

~~TOP SECRET~~

~~CORONA TALENT KEYHOLE NOFORN~~



5.6 LENS FOCUS

The difficulties experienced with the focus adjustments of the panoramic cameras have been discussed in detail in the performance reports for missions 1101, 1102, and 1103.

A careful review of Section 2.0 of these reports should be highly pertinent to the discussion of the present section.

The focus problem has two facets:

1. The position of the focal plane with respect to a mechanical reference on the lens assembly must be determined for the environmental conditions of the mission.
2. Since there is an infinite number of image planes within the depth of focus of the lens, the focal plane must be selected from the image planes so that the performance of the lens is optimized. In addition, the focal plane must be defined in such a way that it can be determined by laboratory measurements or tests.

In the laboratory, the performance of a panoramic camera at various lens focus positions is examined by conducting dynamic resolution tests. From these tests one can plot a curve of dynamic resolution versus focus position. This curve essentially defines the focal plane.

It was originally assumed that the film position should be adjusted to coincide with the peak of the resolution curve. This assumption implies that at the focus position at which the resolution reaches a peak, the MTF of the lens is optimum. Several theoretical investigations conducted by the contractor showed that this assumption was not necessarily true for the Petzval lenses.

In fact, for second generation lenses, the focus position which maximizes the area under the MTF curve is expected to be approximately 0.0005 inch further away from the field flattener element of the lens than the peak of the low contrast resolution curve. It must be pointed out, however, that lenses of the same generation are different from each other, so that one cannot make assumptions as to the focal position of the optimum lens MTF with respect to the resolution versus focus curve. In order to eliminate this uncertainty, the contractor has developed an experimental method which allows one to determine the focal position at which the MTF of a lens is optimum. The method consists of performing dynamic resolution tests in the contractor's laboratories at various focal positions and with various amounts of image smear artificially introduced.

At each focal position of the lens, a dynamic resolution versus image smear curve is obtained. These curves show how the dynamic resolution of the camera is affected by image smear. Since the ability of the camera to withstand a certain amount of image smear with a minimum loss in resolution depends on the focal position occupied by the film, these curves immediately show which focal position results in an image quality least susceptible to image smear, or, essentially, the focal position for which the MTF of the lens has maximum modulation over a large spatial frequency range.

The contractor has conducted dynamic resolution versus image smear and focus tests on all J-3 systems except systems 1101 through 1104. The results of these tests are being reduced and will provide the only reliable information concerning the optimum focal plane.

The only remaining focusing difficulty arises from the ambiguity of the focal plane location during the mission. This ambiguity exists because the focal plane of a lens is established under ambient conditions and the vacuum and thermal environments of the mission produce shifts to the focal plane.

~~TOP SECRET~~

~~CORONA TALENT KEYHOLE NOFORN~~



Handle Via

~~TALENT KEYHOLE~~

Control Systems Jointly

~~TOP SECRET~~

~~CORONA TALENT-KEYHOLE NOFORN~~

The Petzval lenses are known to have nominal air-to-vacuum focus shifts of 0.014 inch. However, static resolution tests in vacuum showed that the air-to-vacuum focus shifts may vary as much as 0.001 inch between various lenses. In addition, the thermal environment results in focus shifts in the order of 0.0005 inch.

The contractor has studied the air-to-vacuum and thermal focus shifts both experimentally and theoretically. The results appear in several reports 6, 7, 8, and 9. After examining the findings of these reports, one concludes that the only dependable method of dealing with these focus shifts is as follows:

1. The difficulties with the air-to-vacuum focus shift can be eliminated by focusing the panoramic cameras dynamically in vacuum.
2. The thermal focus shifts can be minimized by insulating the lens thermally.

Some experience of focusing the panoramic cameras has been gained from the results of missions 1101, 1102, 1103, and 1104. Specifically, the cameras for missions 1102 and 1104 appeared to be properly focused as evidenced from the photographic record. However, there is no certainty that they were optimally focused since only relatively large focusing errors can be detected in the photographic record.

5.7 ATMOSPHERIC EFFECTS

The atmosphere plays a very important role in the performance of the panoramic system. It affects the spatial frequency response of a lens and the contrast of the photography.

5.7.1 Atmospheric MTF

The effect of the atmosphere on the spatial frequency response of a lens can be described by a modulation transfer function (MTF) which is dependent on the altitude of photography, the weather conditions, the aperture and focal length of the optics, and the wavelength of light.

The atmosphere reduces the spatial frequency response of a lens by imposing random wavefront distortions to the plane wavefront of light entering the lens. These wavefront distortions are due to inhomogeneities (density variations) in the air mass through which a beam of light propagates before it reaches the lens. The density variations result in random localized variations in the refractive index of air which tend to speed up or slow down the wavefront and therefore distort it.

Thus, photographing ground targets through the atmosphere is equivalent to photographing targets with a collimator that has aberrations.

The shape of the atmospheric MTF is not known. In the unclassified literature, two articles by D. L. Fried^{6,7} show a mathematical derivation of the atmospheric MTF. Essential to this derivation are:

1. A model of the refractive index covariance function describing the statistics of the refractive index of inhomogeneous air
2. A model of the variation in the statistics of the refractive index with altitude.

Obviously there is a need to measure the wavefront distortions produced by the atmosphere by experimentally utilizing lasers and satellites. In any case, this mathematical derivation shows that the atmospheric MTF behaves in a manner similar to what is expected. In other words, the

~~TOP SECRET~~

~~CORONA TALENT-KEYHOLE NOFORN~~

Handle Via

~~TALENT-KEYHOLE~~

Control Systems Jointly

5-11

~~TOP SECRET~~

~~CORONA TALENT-KEYHOLE NOFORN~~

atmospheric MTF suppresses the high spatial frequencies more severely as the focal length increases and the f /number decreases (the aperture increases for a fixed focal length). On the other hand, the atmospheric MTF improves with increasing altitude for satellite-borne optics of fixed focal length and aperture because the farther the optics are displaced from the inhomogeneous medium (atmosphere), the smaller the wavefront distortion produced by the medium. However, for a fixed ground resolved distance requirement, the atmospheric MTF becomes worse with increasing altitude because the aperture and focal length of the optics increase.

In addition, the mathematical derivation shows that the atmospheric MTF has a negligible effect on the performance of the Petzval lenses. Due to the small aperture (under 7 inches) of the Petzval lenses, one would not expect a major degradation in the performance of the lenses resulting from the atmosphere.

5.7.2 Atmospheric Loss of Contrast

The major degrading effect of the atmosphere on the performance of the panoramic cameras is the reduction in the contrast of the photography. Low contrast implies a weak "signal" and a corresponding low signal-to-noise ratio. Due to the low signal-to-noise ratio, a low contrast image would appear grainier than a higher contrast image. A low signal-to-noise ratio is undesirable because a greater portion of the information available in the image is corrupted by the grain noise of the film.

The loss in contrast due to the atmosphere is partially compensated by using yellow, orange, or red filters (Wratten no. 21, 23A, or 25 filters). Red filters provide better contrast than yellow filters. However, the improvement in contrast is obtained at the expense of intensity of illumination. (Red filters require longer exposure times than yellow filters.) Also, the information available in the spectral regions eliminated by the filter is lost.

The loss in contrast produced by the atmosphere is not constant, but varies with the weather conditions, haze, and smog.

From the Crystal Ball program it has been determined that the contrast factor varies by a factor of 2 between light and heavy haze conditions. Specifically, the contrast factor varies approximately between 10 and 20, corresponding to an atmospheric luminance which is approximately equivalent to a 10 to 20 percent reflectance of sunlight. Unfortunately, these contrast factor values have been computed from photometric units assuming no filters. The information that would be useful for the panoramic cameras is the contrast factor as a function of the wavelength of light determined from radiometric units. Since the contrast of the photography improves when yellow or red filters are used, one expects the contrast factor to be significantly reduced by these filters. However, the contrast factor probably varies approximately by a factor of 2 regardless of the filter being used and depends on the prevailing haze conditions.

The CORN targets utilized in every mission contain an edge target of known reflectances. It is then possible from the image of the edge target to determine the loss in contrast produced by the atmosphere on any other target of known reflectance values. The mathematical treatment of this method is described in Section 3.1 of the 1101 performance evaluation report. One application of this method is the determination of the apparent contrast of resolution targets (part of the CORN displays) as seen through the atmosphere. These targets have a nominal contrast on the ground of 4.7:1. However, their contrast is reduced when photographed through the atmosphere. For missions 1101, 1102, 1103, and 1104, the apparent contrast of the resolution targets varied between 1.5:1 to 2.5:1 for the primary filters (Wratten no. 21 for the AFT-looking camera and Wratten no. 25 for the FWD-looking camera). The variation in apparent contrast was attributed to haze or weather conditions.

~~TOP SECRET~~

~~CORONA TALENT-KEYHOLE NOFORN~~

Handle Via

~~TALENT-KEYHOLE~~

Control Systems Jointly

~~TOP SECRET~~

~~CORONA TALENT-KEYHOLE-NOFORN~~

The conclusions that should be drawn from this discussion are:

1. The atmosphere affects the photographic contrast.
2. The reduction in contrast due to the atmosphere is not constant, but varies significantly with the prevailing haze conditions.

It has also been observed that the changes in the contrast of the photography due to the atmosphere are many times subtle and can be confused with lens defocus or image smear. This is probably due to the fact that the Petzval lens has a narrow field of view in the along-track direction and to the primary filters. In fact, haze is less obvious when the deep red filters are used instead of the yellow filters, and this is another indication of the higher haze-penetrating property of the red filters. On the other hand, haze and loss of contrast due to haze are more obvious in the index camera.

Haze plays a very important role in contrast and thus the information content of the photography. Therefore, accurate forecasting of haze conditions over the targets to be photographed during a mission is almost as important as determining accurately the V/h rate of the vehicle.

5.8 EXPOSURE TIME REQUIREMENTS, IMAGE SMEAR, AND FILTERS

The first priority targets for several missions were found to be located at an average north latitude of 50 degrees. The dispersion of these targets about this average latitude has a standard deviation of approximately 7 degrees. It is well known that the northern latitudes are associated with low solar elevations, especially during the winter months. In turn, low solar elevations result in poor solar illumination of the target areas, and long exposure times are required to achieve a certain exposure level of the film in units of meter-candle-seconds. However, image smear increases linearly with exposure time, and a significant loss in average camera performance should be expected due to image smear for exposure times longer than 4 milliseconds. The loss in performance will be more noticeable in a FWD-looking camera if it is equipped with a III generation Petzval lens and a Wratten no. 25 filter. Therefore, a loss in performance should be anticipated for low solar elevation photography. However, this loss in performance can be minimized by proper selection of filters. Yellow or orange filters (Wratten no. 15 or 21) can be employed in order to reduce the exposure times that would be otherwise needed for a red filter (Wratten no. 25). However, one should remember that the apparent contrast of a target as seen through a yellow or an orange filter is lower than its apparent contrast as seen through a red filter (see Section 5.7.2). In addition, the MTF of a III generation Petzval lens is poorer for filters other than a Wratten no. 25 (see Section 5.5). Therefore, when selecting a filter, one must balance the loss in performance due to image smear (which affects mainly the high spatial frequencies) against the loss in performance due to a poor lens MTF and the lower apparent contrast associated with filters which transmit a broader spectral band of light than the Wratten no. 25 filter.

From Section 5.5 it appears that the MTF of a second generation Petzval lens is approximately the same for the following Wratten filters: nos. 21, 23A, and 25. For a III generation Petzval, the lens MTF is affected by the various filters as follows:

1. The MTF is optimum for a Wratten no. 25 filter.
2. There is a slight loss in performance for a Wratten no. 23A filter.
3. There is a larger reduction in performance for a Wratten no. 21 filter, but to a performance level slightly higher than the performance of a II generation lens with a Wratten no. 21 filter.

~~TOP SECRET~~

~~CORONA TALENT-KEYHOLE-NOFORN~~

Handle Via

~~TALENT-KEYHOLE~~

Control Systems Jointly

~~TOP SECRET~~

~~CORONA TALENT KEYHOLE NOFORN~~

From experience derived from the photography of previous missions, the contractor believes that the atmospheric luminance is higher for the FWD-looking camera than for the AFT-looking camera. Therefore, a slightly more red filter should be utilized in the FWD-looking camera. The recommended filter combinations are as follows:

1. Wratten no. 21 in AFT-looking and Wratten no. 23A in FWD-looking camera
2. Wratten no. 23A in AFT-looking and Wratten no. 25 in FWD-looking camera.

The second combination should be utilized for normal or medium haze conditions, and the first combination should be utilized for very clear weather conditions (i.e., desert areas or haze-free northern latitudes during the winter months).

In any case, use of the maximum slit (0.340 inch) should be avoided. This slit results in exposure times between 4 and 5 milliseconds. The exposure time should be maintained below 4 milliseconds by selecting a filter which transmits a broader spectral band. In comparison with a Wratten no. 25 filter:

1. The Wratten no. 23A filter requires approximately 18 percent less exposure time.
2. The Wratten no. 21 filter requires approximately 33 percent less exposure time.

5.9 LONG-TERM MISSION EFFECTS

As the missions become longer, various problems are expected to arise. Obviously, the lifetime requirements for all the components of a system will be extended. In addition, there is a need to study the long-term effects of the space environment on the system components. Some of the items to be investigated include:

1. Long-term vacuum effects on lubricants and bearings.
2. Long-term effects of penetrating space radiation on semiconductors and the film. The fog level of the film is expected to increase for long missions.
3. Effects of the space environment on the antireflection coatings of optical surfaces.
4. Accumulation of dirt on the exposed optical surfaces.

Items 3 and 4 are related to a satellite problem that was discovered by NASA, i.e., a satellite is surrounded by its own weak atmosphere of particles. The particles may be ions, atoms, molecules, or much larger particles. Most of the particles are thought to originate in the satellite itself from various possible sources:

1. Purging of fuel tanks
2. Evaporation of silicone oils contained in silicone compounds
3. Evaporation from batteries and fuel cells
4. Evaporation of water from the film
5. Nitrogen from the pressure makeup systems
6. Burnt fuel particles and ions from the drag makeup system.

The physical mechanisms by which the particle atmosphere surrounds and follows the satellite may be one or more of the following:

1. The particles have velocities and orbits identical to the velocity and orbit of the satellite.
2. The satellite has a weak gravitational field.

~~TOP SECRET~~

~~CORONA TALENT KEYHOLE NOFORN~~

Handle Via

~~TALENT KEYHOLE~~

Control Systems Jointly

~~TOP SECRET~~

~~CORONA TALENT-KEYHOLE NOFORN~~

3. The satellite probably acquires an electric surface charge because of its motion through the ionosphere.

The mechanisms by which particles escape the satellite atmosphere may be one or both of the following:

1. The particles acquire velocities different than the velocity of the satellite. This, for example, occurs when a drag makeup rocket is fired and the satellite acquires a higher orbital velocity.
2. Atmospheric drag forces may sweep some particles away from the satellite atmosphere.

The density and composition of the satellite atmosphere is important because it affects the camera system performance in two ways:

1. There is a loss in contrast in the photography because the particles diffract sunlight. Due to the low density of the satellite atmosphere, it is expected that only relatively large particles (sizes in the order of a fraction of a micron or larger) would be important to this diffraction process.
2. The satellite atmosphere would tend to deteriorate the exposed optical surfaces either by accumulation of dirt on these surfaces or by erosion of the antireflection coatings. Both effects will reduce the contrast of the photography.

In conclusion, for long missions it is important to determine at least three aspects of the satellite atmosphere problem.

1. The density and composition of the satellite atmosphere should be determined as functions of time in the orbit.
2. The accumulation of dirt on exposed optical surfaces with time should be investigated.
3. The condition of the antireflective coatings with time should be evaluated.

In any case, it seems that long missions would require a method to cover the exposed optical surfaces during the time intervals that the optical system is not being used.

5.10 INTEGRATED GRD

It is not difficult for camera systems to meet certain GRD requirements when no other requirements are simultaneously imposed. A given GRD requirement can be met by most cameras by reducing the altitude of photography. A cursory review of photographic systems of the past shows that two general types have been produced:

1. Camera systems of relatively low GRD performance but large area coverage (search and surveillance systems).
2. Camera systems of large focal lengths and high GRD performance but of limited area coverage (spotting systems). Of course, these systems could cover a large area after a long enough time period.

Therefore, it appears that GRD is not a basic limitation of camera systems; rather, the basic limitation is the information capacity per unit of operating time, or the information capacity

~~TOP SECRET~~

~~CORONA TALENT-KEYHOLE NOFORN~~

Handle Via

~~TALENT-KEYHOLE~~

Control Systems Jointly

5-15

~~TOP SECRET~~

~~CORONA TALENT-KEYHOLE NOFORN~~

per frame. The actual information capacity of a camera system is difficult to compute. However, one could determine another quantity which is the two-dimensional integral of GRD, as follows:

$$I_G = \iint \frac{d_x d_y}{R_x R_y} \quad (5.1)$$

where I_G = integrated GRD per frame in resolution elements (dimensionless units)

R_x = ground resolved distance in cross-track direction

R_y = ground resolved distance in along-track direction

A resolution element is the product of two orthogonal line pairs. The integration is taken over the ground area covered by one frame. x and y are ground coordinates for this area and both R_x and R_y are functions of x and y . An approximate determination of I_G defined by Equation (5.1) can be obtained for the J-3 systems from the following observation.

At an altitude of 85 nm, the new area covered per frame (does not include overlap between adjacent frames) is approximately 1,000 square nm. The average GRD is approximately 9 feet. Multiplying the new area covered per frame by the inverse of the square of the average GRD, one obtains approximately 4.6×10^8 resolution elements per frame, or 2.3×10^8 resolution elements per second. For a full load of 3404 film (approximately 6,000 frames), the integrated GRD is approximately 2.8×10^{12} resolution elements per mission or 1.8×10^{11} resolution elements per day for a 15-day mission.

If, for purposes of discussion, one were to combine the surveillance and spotting requirements into one system such that it has the same area coverage as the J-3 system but at an average GRD of 2 feet, this new system would have an integrated GRD approximately 20 times larger than that of the J-3 system.

~~TOP SECRET~~

~~CORONA TALENT-KEYHOLE NOFORN~~

Handle Via

~~TALENT-KEYHOLE~~

Control Systems Jointly

~~TOP SECRET~~

~~CORONA TALENT-KEYHOLE-NOFORN~~



6. CONCLUSIONS

The CORN target readings and the predictions obtained from the computer resolution prediction program (BLUR Program) are in general agreement (see Tables 4-1 through 4-6) if one takes into account the uncertainties in the focusing conditions of the panoramic cameras and the actual contrast of the CORN targets as seen through the atmosphere. Undoubtedly, there are errors in the BLUR Program (the accuracy of the resolution predictions is estimated as between 10 and 20 percent), but the contractor is confident that this computer program on the average describes very well the performance of the J-3 systems. In addition, the BLUR Program is extremely useful in understanding the influence of the various parameters on system resolution performance. The program has already been used in several investigations into the performance of the J-3 systems (other than the resolution predictions for CORN and first priority targets described in References 1 through 4). Comparison of the BLUR Program with the nominal image smear budgets (Tables 3-1 and 3-2) reveals the following:

1. The actual image smear in the along-track direction should be about 1.5 times larger than that anticipated by the budget. This is due primarily to a camera torsional vibration frequency (see Section 5.3). The along-track image smear is generally small and produces a significant reduction in along-track resolution only for exposure times longer than 3 milliseconds.

2. The actual image smear in the cross-track direction averaged over the panoramic format appears to be about equal to the average cross-track image smear predicted by the budget. The distribution over the format of this image smear should be similar to Figs. 5-1 and 5-2.

In general, the contractor feels that the panoramic cameras of systems CR-2 and CR-4 have met the specifications described in the error budgets (Tables 3-1 through 3-4). (The resolution performances of systems CR-1 and CR-3 were reduced due to an unexpected focus shift.)

Other conclusions drawn from this report are:

1. The third generation Petzval lens is an extraordinary improvement over the second generation one (see Section 5.5).

2. Focusing of the panoramic cameras for the mission environment is still a difficult task. The resolution tests conducted at various focal positions and artificially introduced image smears provide extremely valuable data for focusing the cameras (see Section 5.6).

3. The concept of integrated GRD defined in Section 5.10 is a useful and practical quantity which describes the ability of a camera system to record information. It takes into account the GRD performance of a system as well as its area coverage and can be used for comparing different camera systems.

~~TOP SECRET~~

~~CORONA TALENT-KEYHOLE-NOFORN~~



Handle Via

~~TALENT-KEYHOLE~~

Control Systems Jointly



7. REFERENCES


1. [REDACTED] performance Analysis Report for Mission 1101, [REDACTED] (1 Feb 1968).
2. [REDACTED] Performance Analysis Report for Mission 1102, [REDACTED] (3 June 1968).
3. [REDACTED] Performance Analysis Report for Mission 1103, [REDACTED] (20 Dec 1968).
4. [REDACTED] Performance Analysis Report for Mission 1104, [REDACTED] (2 Apr 1969).
5. J-3 Panoramic Camera System, Description and Operation Manual [REDACTED]
6. Fried, D. L., Optical Resolution Through a Randomly Inhomogeneous Medium for Very Long and Very Short Exposures, JOSA, 56(10):1,372 (Oct 1966).
7. Fried, D. L., Limiting Resolution Looking Down Through the Atmosphere, JOSA, 56(10):1,380 (Oct 1966).
8. Cobb, M., Williams, T., Voggenthaler, J., Second Series of Test Results (Petzval 3); Project 9624.07A (23 Jan 1968).
9. Cobb, M., Voggenthaler, J., Transient and Off-Axis Petzval Lens Cell Thermal/Optical Test Program Final Report No. 253 (Oct 1968).
10. Monroe, G. A., Flight Data Thermal Analysis Report—CR-5, Project 9232.17 (Jan 1969).



Appendix

VEHICLE ERROR ANALYSIS FOR PANORAMIC CAMERAS

The image velocities in a panoramic camera which result from errors in the orientation of the vehicle as well as the rate of change of orientation and the relative motion of the vehicle with respect to the earth are derived below.

We start with the basic transformation equations between ground coordinates and panoramic camera format coordinates. The transformation equations were derived by  on the assumption that the earth's surface is flat. This is a good approximation for altitudes up to 500 nm and for average scan angles (± 45 degrees). The symbols used throughout this appendix and applicable illustrations are presented in the addendum.

The basic transformation equations are:

$$X = h \left(\frac{f \cos \theta \sin \phi + x \cos \phi}{f \cos \theta \cos \phi - x \sin \phi} \right) \quad (1)$$

$$Y = \frac{hf \sin \theta}{f \cos \theta \cos \phi - x \sin \phi} \quad (2)$$

From these equations, by rearrangement and substitutions, we obtain:

$$x = \frac{f \cos \theta \left(\frac{X}{h} - \tan \phi \right)}{1 + \frac{X}{h} \tan \phi} \quad (3)$$

and

$$y = f \arctan \left(\frac{\frac{Y}{h}}{\cos \phi + \frac{X}{h} \sin \phi} \right) \quad (4)$$

~~TOP SECRET~~

~~CORONA TALENT-KEYHOLE NOFORN~~

The derivatives of equations (3) and (4) are:

$$\dot{x} = \frac{-f\dot{\theta} \sin \theta \left(\frac{X}{h} - \tan \phi \right)}{1 + \frac{X}{h} \tan \phi} + \frac{f \cos \theta \sec^2 \phi \left[\frac{\dot{X}}{h} - \dot{\phi} \left(1 + \frac{X^2}{f^2} \right) \right]}{\left(1 + \frac{X}{h} \tan \phi \right)^2} \quad (5)$$

and

$$\frac{\dot{y}}{f} = \frac{\left(\cos \phi + \frac{X}{h} \sin \phi \right) \frac{\dot{Y}}{h} - \frac{Y}{h} \left(\frac{X}{h} \dot{\phi} \cos \phi + \frac{\dot{X}}{h} \sin \phi - \dot{\phi} \sin \phi \right)}{\left(\cos \phi + \frac{X}{h} \sin \phi \right)^2 + \frac{Y^2}{f^2}} \quad (6)$$

Now, equations (1) and (2) are substituted for X and Y into equations (5) and (6). Then,

$$\dot{x} = -\dot{\theta} x \tan \theta + \frac{1}{f \cos \theta} \left[\frac{\dot{X}}{h} (f \cos \theta \cos \phi - x \sin \phi)^2 - \dot{\phi} (x^2 + f^2 \cos^2 \theta) \right] \quad (7)$$

and

$$\dot{y} = (f \cos \theta \cos \phi - x \sin \phi) \left(\frac{\dot{Y}}{h} \cos \theta - \frac{\dot{X}}{h} \sin \phi \sin \theta \right) - x \dot{\phi} \sin \theta \quad (8)$$

Since, $x \ll f$ in most cases, the second order term $(x/f)^2$ may be eliminated, and equation (7) becomes approximately:

$$\dot{x} \approx -\dot{\theta} x \tan \theta + \frac{\dot{X}}{h} (f \cos \theta \cos^2 \phi - x \sin 2\phi) - f \dot{\phi} \cos \theta \quad (9)$$

We will now derive \dot{X} and \dot{Y} as functions of x , ϕ , θ , V_T , α , $\dot{\alpha}$, and $\dot{\theta}$. Second order terms involving cross-products of small errors will be neglected. It is assumed that α , $\dot{\alpha}$, θ , $\dot{\theta}$, ϕ , ρ , $\dot{\rho}$, θ_ϵ , and ϕ_ϵ are all small errors.

From trigonometric principles, we find that:

$$\phi_\epsilon \approx \beta \quad (\text{definition}) \quad (10)$$

$$\dot{\phi} = \dot{\phi}_\epsilon \approx \dot{\beta} \quad (11)$$

$$\tan \theta_\epsilon = \cos \phi \tan \rho \quad (12)$$

$$\dot{\theta} = \dot{\theta}_\epsilon \approx \dot{\rho} \cos \phi \quad (13)$$

$$\begin{aligned} \dot{X} &= -V_T \cos (\alpha + \rho \tan \phi) + \dot{\alpha} Y \\ &\approx -V_T + \frac{\dot{\alpha} h \tan \theta}{\cos \phi} \left(1 + \frac{x \tan \phi}{f \cos \theta} \right) \end{aligned} \quad (14)$$

~~TOP SECRET~~

~~CORONA TALENT-KEYHOLE NOFORN~~



Handle Via
~~TALENT-KEYHOLE~~
Control Systems Jointly

~~TOP SECRET~~

CORONA ~~TALENT-KEYHOLE-NOFORN~~



$$\dot{Y} = -V_T \sin(\alpha + \rho \tan \phi) + \dot{\theta} \left(\frac{\partial Y}{\partial \theta} \right) + \dot{\alpha} X \tag{15}$$

$$\approx -V_T(\alpha + \rho \tan \phi) + \frac{h \dot{\theta} \left(1 + \frac{x}{f} \tan \phi \right)}{\cos \phi \cos^2 \theta} + h \dot{\alpha} \tan \phi \left(1 + \frac{2x}{f \cos \theta \sin 2\phi} \right)$$

We now substitute equations (14) and (15) into equations (8) and (9) and we obtain:

$$\dot{x} \approx -\dot{\rho} x \cos \phi \tan \theta - f \dot{\phi} \cos \theta + \dot{\alpha} (f \sin \theta \cos \phi - x \sin \phi \tan \theta) - \frac{f V_T}{h} \left(\cos \theta \cos^2 \phi - \frac{x}{f} \sin 2\phi \right) \tag{16}$$

$$\dot{y} \approx (f \cos \phi \cos \theta - x \sin \phi) \left[-\frac{V_T}{h} (\alpha + \rho \tan \phi) \cos \theta + \frac{V_T}{h} \sin \phi \sin \theta \right] + f \dot{\rho} \cos \phi + x \dot{\rho} \frac{\sin \phi}{\cos \theta} (\cos \theta - 1) + x \dot{\alpha} \frac{\cos \theta}{\cos \phi} + f \dot{\alpha} \sin \phi \cos 2\theta \tag{17}$$

Equations (16) and (17) are actually approximations assuming that $\theta_{\max} < 90$ degrees, $x/f \ll 1$, and $\phi < 18$ degrees. Terms involving $\sin^2 \phi$, $(x/f)^2$, and $\tan^2 \phi$ were neglected. To be more correct, ϕ and θ in equations (16) and (17) should be replaced by $(\phi + \phi_\epsilon)$ and $(\theta + \theta_\epsilon)$, respectively. However, taking into account the magnitudes of the different components in equations (16) and (17), we find the only terms which are affected appreciably are:

$$-\frac{f V_T}{h} \left(\cos \theta \cos^2 \phi - \frac{x}{f} \sin 2\phi \right) \quad \text{[in equation (16)]}$$

and

$$(f \cos \phi \cos \theta - x \sin \phi) \frac{V_T}{h} \sin \phi \sin \theta \quad \text{[in equation (17)]}$$

These terms must be corrected. Therefore,

$$-\frac{f V_T}{h} \left[\cos(\theta + \theta_\epsilon) \cos^2(\phi + \phi_\epsilon) - \frac{x}{f} \sin 2(\phi + \phi_\epsilon) \right] \approx -\frac{f V_T}{h} \left[\cos \theta \cos^2 \phi - \rho \cos^3 \phi \sin \theta - \beta \sin 2\phi \cos \theta - \frac{x}{f} (\sin 2\phi + 2\beta \cos 2\phi) \right] \tag{18}$$

and

$$\frac{f V_T}{h} \left[\frac{1}{4} \sin 2(\phi + \phi_\epsilon) \sin 2(\theta + \theta_\epsilon) - \frac{x}{f} \sin^2(\phi + \phi_\epsilon) \sin(\theta + \theta_\epsilon) \right] \approx \frac{f V_T}{h} \left[\frac{1}{4} \sin 2\phi \sin 2\theta + \frac{1}{2} \beta \cos 2\phi \sin 2\theta + \rho \cos^2 \phi \sin \phi \cos 2\theta - \frac{x}{f} (\sin^2 \phi \sin \theta + \beta \sin 2\phi \sin \theta) \right] \tag{19}$$

~~TOP SECRET~~

CORONA ~~TALENT-KEYHOLE-NOFORN~~

~~TALENT-KEYHOLE~~

Handle Via
Control Systems Jointly

~~TOP SECRET~~

~~CORONA TALENT KEYHOLE NOFORN~~

We now substitute equations (18) and (19) into equations (16) and (17), respectively, to obtain the final results.

$$\dot{x} \approx -\dot{\rho} x \cos \phi \tan \theta - f \dot{\phi} \cos \theta + \dot{\alpha} (f \sin \theta \cos \phi - x \sin \phi \tan \theta) - \frac{fV_T}{h} \left[\cos \theta \cos^2 \phi - \rho \cos^3 \phi \sin \theta - \beta \sin 2\phi \cos \theta - \frac{x}{f} (\sin 2\phi + 2\beta \cos 2\phi) \right] \quad (20)$$

$$\begin{aligned} \dot{y} \approx & - (f \cos \phi \cos \theta - x \sin \phi) \frac{V_T}{h} \cos \theta (\alpha + \rho \tan \phi) + f \dot{\rho} \cos \phi \\ & + x \dot{\rho} \frac{\sin \phi}{\cos \theta} (\cos \theta - 1) + f \dot{\alpha} \sin \phi \cos 2\theta + x \dot{\alpha} \frac{\cos \theta}{\cos \phi} \\ & + \frac{fV_T}{h} \left[\frac{1}{4} \sin 2\phi \sin 2\theta + \frac{1}{2} \beta \cos 2\phi \sin 2\theta + \rho \cos^2 \phi \sin \phi \cos 2\theta \right. \\ & \left. - \frac{x}{f} (\sin^2 \phi + \beta \sin 2\phi) \sin \theta \right] \quad (21) \end{aligned}$$

~~TOP SECRET~~

~~CORONA TALENT KEYHOLE NOFORN~~

Handle Via

~~TALENT KEYHOLE~~

Control Systems Jointly



Addendum

FIGURES AND SYMBOLS

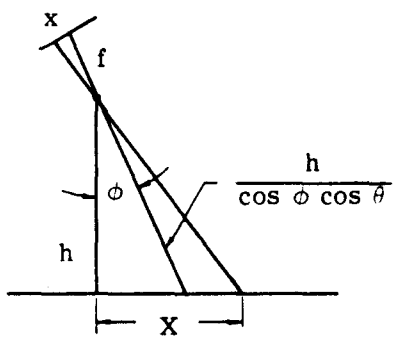


Fig. A-1 — X definition

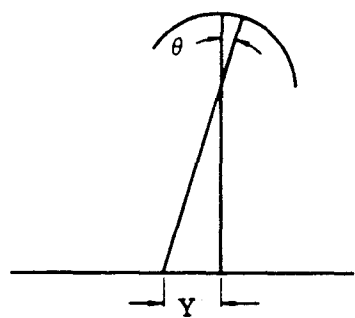


Fig. A-2 — Y definition

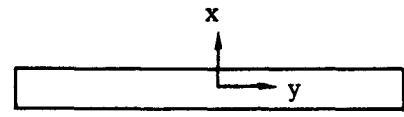


Fig. A-3 — Panoramic camera format

X and Y are ground distances defined above

- h = altitude
- f = focal length
- θ = scan angle ($y = f\theta$)
- ϕ = half stereo angle
- x and y = format distances

- α = yaw error angle
- ρ = roll error angle
- β = pitch error angle
- θ_{ϵ} = scan angle error
- ϕ_{ϵ} = half stereo angle error
- T = period of a circular orbit

V_T = velocity of the ground with respect to the vehicle. When no vehicle orientation and rate errors exist, V_T has the direction of $-\dot{X}$